EXPLORATION OF 3D PRINTING A NEW POLYSILOXANE COMPOSITE FOR HIGH TEMPERATURE APPLICATIONS

by

William Josef Schneider, B.S.

A thesis submitted to the Graduate Council of
Texas State University in partial fulfillment
of the requirements for the degree of
Master of Science
with a major in Engineering
December 2019

Committee Members:

Jitendra Tate, Chair

Austin Talley

Emily Hacopian

Stan Bouslog

FAIR USE AND AUTHOR'S PERMISSION STATEMENT

Fair Use

Duplication Permission

DEDICATION

I would like to dedicate this work to Brenda Schneider and Katherine Montez, my grandmothers. Their guidance, support and unconditional love gives me motivation every day to achieve things that I never imagined possible for myself.

ACKNOWLEDGMENTS

The M.S. Engineering program at Texas State has given me everything and more than I could have hoped for. The hands-on experience with cutting edge manufacturing techniques have given me the ability to pursue career and personal opportunities that I never would have imaged before attending. For this, I would like to thank Texas State University, The Graduate College, and the Ingram School of Engineering.

This research could not have been done without the guidance of my advisors and members of the Texas State faculty. I am extremely grateful to Dr. Tate for giving me the opportunity to work in his lab and for his mentoring during my research journey. I would also like to thank Dr. Austin Talley for his advice and wisdom that goes beyond this research, he is an excellent example of what a teacher should strive to be. Dr. Emily Hacopian and Mr. Stan Bouslog of NASA JSC have been extremely supportive throughout this process and without their blessing this research could not have been initiated.

For the use of their time and resources, I would like to thank Dr. Bahram Asiabanpour, Dr. Namwon Kim, the Ingram Hall Makerspace and Texas Research Institute. Lastly, I would like to thank Swayam Shree, Harish Kallagunta, Zane Gooden and the members of the Advanced Composites Lab for their constant support and advice from the moment I entered the lab.

TABLE OF CONTENTS

Page

LIST OF TABLES

Table **Page**

LIST OF FIGURES

Figure **Page**

ABSTRACT

Thermal protection materials are a necessary component for high-temperature applications because they serve as protection for delicate components, structures and payloads. Advanced composites are the materials of choice for these applications because of their ability to be fine-tuned for specific parameters. Current thermal protection materials are usually manufactured with fiber reinforced polymer composites. Phenolic resins, specifically SC-1008, are the preferred matrix materials for thermal protection material systems because of their low cost and abundant characterization. Techneglas UHTR resin has recently been explored as a better alternative to phenolic resins and it has vastly outperformed phenolic's thermal properties. Current thermal protection material manufacturing and fabrication processes are very labor intensive and design freedom is limited. There is an inherent need to automate the manufacturing process and create more design flexibility. 3D printing presents a solution to current thermal protection material manufacturing limitations. The goal of this research was to develop and characterize a UHTR composite that can be 3D printed (extruded) into thermal protection for high-temperature applications. The resin was mixed with milled carbon fiber (MCF) and phenolic microballoons (PMB) to form the composite. The initial research was focused on understanding the material system and optimizing it for 3D printing. This involved determining the proper curing mechanism, between multiple catalysts and thermal curing as well as determination of the proper loading levels of the two fillers. A final material system of 10wt% MCF/5wt% PMB was selected because of

its performance during DMA, TGA, and flexural testing. The UHTR resin was tested for UV curability and it was found not to be compatible with UV curing. UHTR uses IPA to control its viscosity and rheological studies were conducted to determine the optimal amount needed for extrusion and it was concluded that 15wt% was ideal for this application. Finally, an auger extruder prototype was developed that was adapted to an off the shelf TAZ LulzBot 3D printer. These fundamental studies will be used as a foundation for future work in UHTR characterization and 3D printing of thermoset resins.

Key Words: Thermal Protection, Polysiloxane, Ablation, 3D Printing, Thermoset

I. INTRODUCTION

Motivation

The space and aerospace industries are on the forefront of materials research out of a necessity for materials with high performance in nontraditional conditions. Thermal protection materials serve as a protective layer for surfaces, delicate components and structures. High-temperature materials are commonly found on aerospace vehicles, such as planetary probes, and spacecraft because of the extreme heat fluxes they endure traveling through planetary atmosphere (Natali, Kenny, & Torre, 2016). High-temperature thermal protection materials have applications with electronics as well. Thermal protection materials are classified as ablative or non-ablative and the latter of which uses re-radiation to protect components and is not destroyed in the process (Natali, Kenny, Torre, 2016).

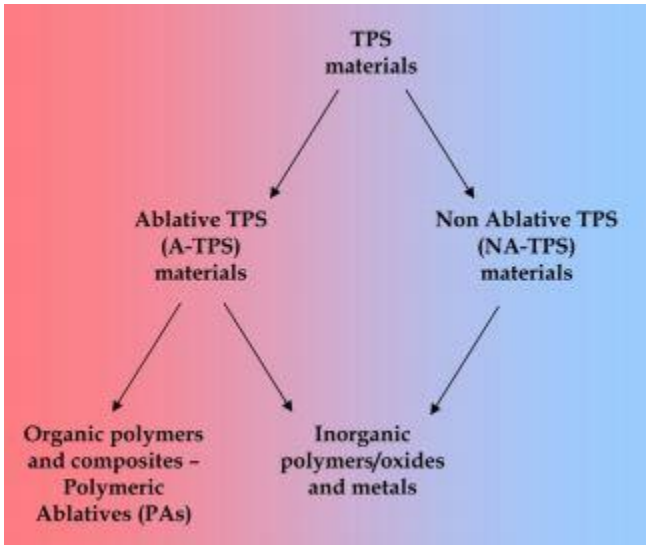

Figure 1 – Ablative and Non-Ablative TPSs (Natali, Kenny, Torre, 2016)

Ablative materials functionally degrade at very high temperatures in a process called pyrolysis. This process results in a porous char layer that insulates the respective

components from high temperatures (Torre, Kenny, Boghetich, & Maffezzoli, 2000). Composites are ideal for thermal protection because of their unique properties that can be manipulated for specific applications. Composite thermal protection materials have high specific strength, good mechanical properties, and heat protection because of physical and chemical changes that can occur when they are introduced to high temperatures (Formalev, Kolesnik, Kuznetsova, & Rabinskii, 2015).

Manufacturing processes using materials for high-temperature applications are usually very manual and inefficient, so there is a motivation for improvement. To manufacture NASA's Orion thermal protection, technicians from Lockheed Martin individually machined 180 unique blocks and secured them to the vessel, a very time-consuming process (Herridge, 2018). Conventional manufacturing methods limit design and process flexibility. Additive manufacturing presents a novel solution that can redefine manufacturing for high-temperature applications because it can automate the process and free up geometric constraints.

Background Information

Ablation Mechanisms in Thermal Protection

Ablation is the functional degradation of a material as it is exposed to high heat fluxes. When an ablative composite material begins to degrade, a pyrolysis layer starts to form and makes its way through the thickness of the material. Eventually, pyrolysis wears off, leaving a porous layer of char on the surface. The char layer serves as the main mode of protection because it acts as an insulator that limits the amount of oxygen reaching the virgin material, deterring exothermic reactions and it protects it from contact

with flames. The char layer also cools the composite due to its ability to slow the release of gases from the pyrolysis layer.

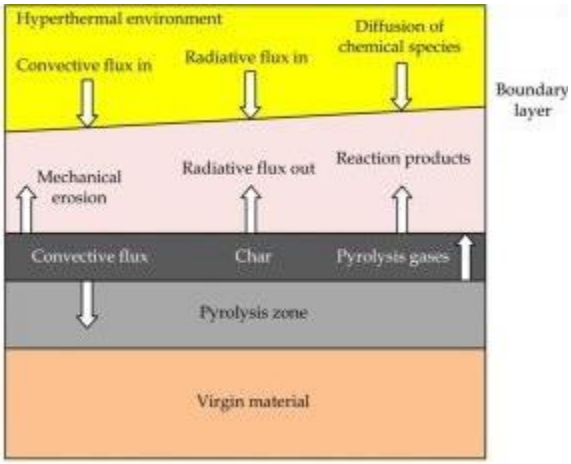

Figure 2 - Charring Polymeric Ablative Diagram

Ablative Polymers

Phenolic resins are widely used in high temperature applications because they are extremely flame resistant and maintain a low toxicity. Phenolics are very well suited for ablative thermal protection applications specifically because they have good thermal stability and high char yield after pyrolysis (Strong, 2008, Silva, Pardini, & Bittencourt, 2016). SC-1008 is a low-cost phenolic resin on the market that is backed by a lot of research, making it a popular choice for high-temperature applications (Schellhase, Koo, Buffy, Wu, & Liu, 2017). Other resins, like cyanate ester, are used in thermal protection applications as well. Cyanate ester was used in various components of NASA's Orion spacecraft (Vitug, 2016). Table 1 summarizes the findings of a review of ablative polymers conducted by NASA. (Boghozian, Stackpoole, & Gonzales, 2015)

Table 1 – Ablative Characteristics of Polymers ***(Boghozian, Stackpoole, & Gonzales, 2015)***

Resin	Decomposition Temperature (°C)	Char Yield (%)
Phenolic	375	49
Cyanate Ester	417	56
Polyimide	529	67
Polybenzoxazine	294	20
Polybenzamidazole	298	52

Techneglas, LLC UHTR is a polysiloxane resin that has recently been gaining traction as a thermal protection polymer matrix. UHTR is a preceramic polymer, a type of polymer that converts to a ceramic via pyrolysis. Schellhase et al. compared the ablation performance of SC-1008 phenolic resin against Techneglas UHTR. The UHTR had a greater char yield, 86.5%, than the SC-1008, 55.4%, which can be observed in Figure 3. UHTR also showed to have a low heat release capacity and a very high heat release temperature, which suggests it has low flammability and is very thermally stable. Overall it outperformed the phenolic SC-1008. (Schellhase, Koo, Wu & Buffy 2018)

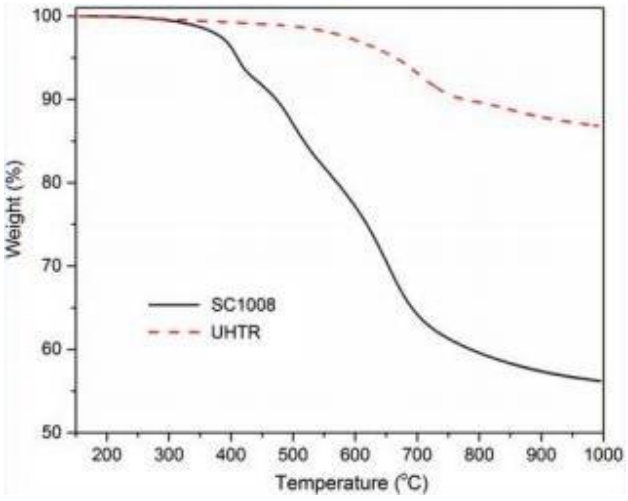

Figure 3 – UHTR & SC-1008 TGA Curves

Low Density Fillers

Ablators composed of polymers exclusively, suffer from weak and brittle char. When ablators degrade, a porous char layer is formed that allows gases to escape and insulates the substrate from high temperatures (Torre, Kenny, Boghetich, & Maffezzoli, 2000). Reinforcement is necessary to improve the mechanical properties of the char, as it needs to withstand the potential forces present in real world environments (Torre, Kenny, Boghetich, & Maffezzoli, 2000). Thermal protection composites commonly use but are not limited to continuous fibers, woven fabrics and core materials for reinforcement. The Orion thermal protection currently uses a glass honeycomb core structure as reinforcement (Clark, 2014). Short fibers made from carbon, glass, boron and dispersed particles like glass microballoons and powders are also great candidates for reinforcement (Dimitrenko, 2018). Characteristics like high aspect ratio, flexibility, and good mechanical properties are what make fibers more attractive reinforcements. More specifically, carbon-based fibers are low density, great thermal conductors and have high tensile strength (Permal et al., 2017). Milled carbon fibers are used to manufacture porous structures that are later impregnated with a phenolic matrix to form phenolic impregnated carbon ablators (PICAs), a thermal protection material used for spacecraft. (Natali, Puri, et al., 2017)

Figure 4 - Zoltek Milled Carbon Fibers

Although they provide some reinforcement, phenolic microballoons are used as low-density fillers to keep the overall density of composites manageable. The high cost of transporting things into space creates the motivation to reduce the weight of thermal protection materials as much as possible and microballoons are a great way to reduce the density for space applications. The heatshield of the Apollo spacecraft was manufactured using Avcoat-5026, an epoxy-phenolic matrix with the addition of silica fibers and phenolic microballoons (Bartlett et al., 1971). Jia et al. used phenolic microballoons to reduce the density of elastomeric heat shielding materials (EHSM) that are used for solid rocket motors. (Jia et al., 2010). Phenolic microballoons are very advantageous for high temperature applications and perform better than glass balloons. As previously stated, phenolic resins are used for ablative thermal protection materials and like the resin, phenolic microballoons will contribute to the char yield of an ablative composite. (Torre, Kenny, & Maffezzoli, 1998)

Thermal Protection Manufacturing

The manufacturing process for thermal protection materials can vary by application, geometry and cost. Current thermal protection materials are manufactured using common composite manufacturing techniques like hand lay-up, compression molding and vacuum infusion. For his thesis research, McDermott used a combination of compression molding and vacuum assisted resin transfer molding (VARTM) to manufacture a UHTR matrix composite (McDermott, 2018). The thermal protection used on the Orion spacecraft uses a honeycomb structure with 330,000 holes that are filled manually one by one with Avcoat material, a process that takes around six months to complete (Clark, 2014).

Manufacturing processes for thermal protection applications are usually very manual with little design flexibility. Additive manufacturing or 3D printing can be a novel approach to high-temperature material fabrication. 3D printing can automate the process and it isn't constrained by geometry like conventional processes. Although they are less common than thermoplastic processes, 3D printing techniques like stereolithography, digital light processing (DLP) and direct ink writing (DIW) can process thermoset resins. Stereolithography and DLP both utilize photosensitive polymers that are held in a vat and selectively cured (Zhang, Jung, 2018). Preceramic polymers in different forms have been explored in several 3D printing processes that are outlined in table 2.

Table 2 – 3D Printing Techniques for Preceramic Polymers (Colombo, Schmidt, Franchin, Zocca, & Gunster, 2017).

Technology	Feedstock	Part Dimension	Surface Quality	Resolution (μm)
Powder 3-D Printing	Powder	M-XL	Medium	100
Inkjet Printing	Liquid	XS-M	High	20
Direct Ink Writing	Paste	M-L	Low	100
Laminated Object Manufacturing	Paste	S-XL	Low	60
Fused Deposition Modeling	Filament	M-XL	Low	100
Stereolithography	Liquid	XS-M	High	25
Two-Photon Photopolymerization	Liquid	XS-S	High	<1

To effectively print a preceramic polymer using DIW, it must have specific rheological characteristics to prevent it from deforming. Polymers have also been dispersed or dissolved into liquids that quickly evaporate after printing which allows the printed material to maintain its shape (Colombo, Schmidt, Franchin, Zocca, & Gunster, 2017). Although these processes have promise, they are not suitable for this application and material.

Goals and Objectives

The ultimate goal of this research is to optimize a polysiloxane resin, that has already proven to have excellent ablative properties, with milled carbon fibers and phenolic microballoons so that it can be 3D printed directly onto a substrate. This research is expected to yield:

- Further characterization on Techneglas LLC. UHTR resin.
- Develop a material system for 3D printing using MCF and PMB.
- Develop a 3D printing prototype using a TAZ LulzBot.

II. MATERIAL SYSTEM DEVELOPMENT

Techneglas, LLC. UHTR

UHTR is a polysiloxane resin for high-temperature applications and its ablative performance has been well supported in literature (Schellhase, Koo, Buffy, Wu, & Liu, 2017). Polysiloxanes are a unique type of inorganic polymer that can convert to ceramic materials through pyrolysis, known as preceramic polymers (Colombo, Schmidt, Franchin, Zocca & Gunster, 2017). UHTR can cure thermally or by using a variety of catalysts. UHTR is available in solid (UHTR-F) and liquid forms (UHTR-IPA). UHTR-IPA is made up of 65% resin solids and 35% isopropyl alcohol, which allows the resin to be at a workable viscosity at room temperature. UHTR is compatible with solvents other than IPA as well. There are also several other formulations of UHTR available, some of which came available after the initiation of this research. Figure 5 shows the properties of Techneglas, LLC. UHTR.

Product Data

Uncured Techneglas UHTR

Appearance	Slightly cloudy liquid
Viscosity	95 cPs
Percent of Solids	65%
Odor (liquid)	Slight Solvent
V.O.C.	368 g/L (3.1 lb/gal)
Density	1.1 g/mL (9.2 lb/gal)
Pot Life at 25°C when catalyzed	1-3 hours
Liquid Ignition Temperature	>300°C

Figure 5 - Properties of Techneglas, LLC. UHTR

Phenolic Microballoons

Currently, it cost upwards of $10,000 to send 1 pound of cargo into space and it is important that weight is reduced in every way possible for these applications. Phenolic microballoons are an ideal low-density filler for ablators because they also contribute to the degradation reaction (Torre, Kenny, & Maffezzoli, 1998). The microballoons used in this research are manufactured by Malayan Adhesives & Chemicals and were provided by NASA. The BJO-0930 Phenoset Microspheres have a density range of 0.21-0.25 g/mL and further properties are listed in figure 6 below.

PHENOSET MICROSPHERES

BJO-0930 hollow microspheres are reddish-brown in colour and primarily used as a hollow filler. The density and maximum working pressure allows the formulator to choose the minimum density product that will survive formulation, pumping and use.

TYPICAL PROPERTIES

Average Hydrostatic Compressive Strength	350 psi
Liquid Density (Liquid Displacement)	0.21 to 0.25 g/mL
Average Bulk Density	0.104 g/cc max
Moisture Content	< 4 wt %
Floatation in Toluene Dupanol solution	> 90 %
Mean Particle Size	90 microns by sieve method 65 microns by laser diffraction

Figure 6 - Phenolic Microballoon Product Data Sheet

Milled Carbon Fiber

For ablative materials, the char layer is vital to their performance as thermal protectors. Neat polymer ablators produce weak and brittle char layers that can be easily removed by mechanical forces introduced during their respective applications, so it is

important to have reinforcement that can mitigate this issue (Torre, Kenny, Boghetich, & Maffezzoli, 2000). Milled carbon fibers are low density and have good mechanical properties, both advantageous characteristics for use in thermal protection materials. The MCFs used for this project are low cost and suitable for aerospace and electronic applications. The milled fibers are processed polyacrylanitrile (PAN) based fibers manufactured by ZOLTEK with an average fiber length between 100-150 µm.

MATERIAL OVERVIEW	PX35		PX30 MF/ME	
	SI	US	SI	US
Carbon Content	95%		99%	
Electrical Resistivity (Volume)	0.00155 ohm-cm	0.00061 ohm-in	0.0017 ohm-cm	0.00055 ohm-in
Linear Resistivity	0.0761 Ω/cm	0.02996 Ω/in	0.069 Ω/cm	0.02717 Ω/in
Density	1.81 g/cc	0.065 lb/in³	1.75 g/cc	0.063 lb/in³
Bulk Density	490 g/L	30.6 lb/ft³	465 g/L (MF150) 350 g/L (MF200)	30.6 lb/ft³ (MF150) 30.6 lb/ft³ (MF200)
Fiber Diameter	7.2 µm	0.283 mils	7.2 µm	0.238 mils
Average Fiber Length	100 µm (MF150) 150 µm (MF200)	4 mils (MF150) 6 mils (MF200)	100 µm (MF150) 150 µm (MF200)	4 mils (MF150) 6 mils (MF200)
Filament Shape	Round			

Figure 7 - Properties of Milled Carbon Fibers

Catalysts

The manufacturer recommends curing UHTR with Titanium (IV) Butoxide at 2-3 wt% and N-(2-Aminoethyl)-3-aminopropyltrimethoxysilane at 1-2 wt%. During discussions with Texas Research Institute - Austin, who has experience with UHTR, they recommended trying BIS(Triethoxysilylpropyl)Amine 95% for comparison with the catalysts the manufacturer lists.

N-(2-Aminoethyl)-3-aminopropyltrimethoxysilane (Geniosil GF 91)

Manufactured by Wacker, Geniosil GF 91 was provided with each order of UHTR. According to the manufacturer, Geniosil GF 91 can improve dispersibility, flexural strength, modulus of elasticity, corrosion resistance and electrical properties.

Titanium (IV) Butoxide

Titanium (IV) Butoxide was the other catalyst recommended by the manufacturer to cure UHTR. The catalyst is manufactured by Sigma-Aldrich and commonly used in thin film applications.

BIS(Triethoxysilylpropyl)Amine 95%

BIS(Triethoxysilylpropyl)Amine 95% is manufactured by Gelest and was used to compare against Techneglas's recommendations.

Initial Experimentation

The initial experiments addressed the issue of UHTR's very short workable life, and the goal was to extend the workable life to 2-3 hours by decreasing the catalyst loading level. The 2-3 hour goal would need to be achieved with the addition of the fillers. Previous research recommended using 20-30wt% of fillers, so these experiments used a total of 30wt%. The scope of work was later altered after the observations made in the initial experiments. These experiments were slightly too ambitious and UHTR needed to be understood more before moving forward. The sections below describe the initial experiments, the results and observations.

Experiment 1 – Catalyst Ratio

The very first experiment was done with neat UHTR resin and the goal was to determine the catalyst ratio that resulted in the longest workable life. This was the important first step to reaching the target of a 2-3 hour pot life. The manufacturer recommends a 100:2 catalyst ratio for the Geniosil GF 91 catalyst. Time, temperature and viscosity were recorded for UHTR mixtures with 4 different catalyst ratios as they were stirred by hand in a beaker. Viscosity was ranked on a scale of 1 to 10 with 8 being unworkable, the viscosity was determined by feel of the person stirring.

Table 3 - Results of Experiment 1

Test	Resin Wt	Catalyst Ratio	Catalyst Wt	Total Wt	Workable Life	Max Temp.
1	25 g	100:1	0.25 g	25.25 g	17 min	26 C
2	25 g	100:0.50	0.125 g	25.125 g	25 min	26 C
3	25 g	100:0.25	0.0625 g	25.0625 g	35 min	27 C
4	25 g	100:0.10	0.025 g	25.025 g	46 min	28 C

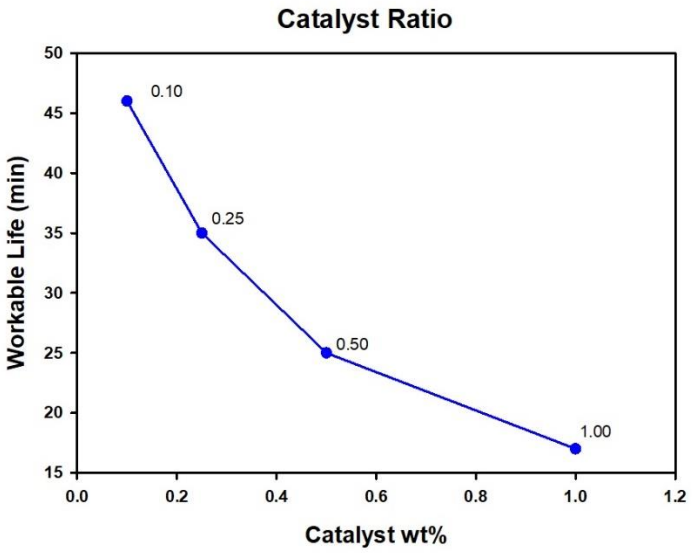

Figure 8 - Results of Experiment 1

A catalyst ratio of 100:0.1 was selected to move forward with based on the results.

Experiment 2 – Workable Life with Fillers

The intention of this research is to develop a composite that can be 3D printed via extrusion. To simulate this process, catheter tip syringes, shown in figure 9 were used because of their accessibility and low cost.

Figure 9 – 60 mL Catheter Tip Syringe

Experiment 2 focused on the effects of adding milled carbon fibers and phenolic microballoons into UHTR with a catalyst ratio of 100:0.1. Initially, viscosity was going to be recorded following the same method used in experiment 1 but viscosity of the composite slurry was hard to gauge by hand. The experiment was altered to accommodate for this and extrudability out of a catheter tip syringe and temperature were recorded at different time intervals. The carbon fiber was added before the microballoons and both were added in 1-gram increments. The mixture was manually stirred with tongue depressors. Table 4 shows the experimental set up.

Table 4 - Experimental Set Up for Experiment 2

Resin	Catalyst	MCFs	PMBs
25g UHTR	0.01 wt% - 0.025g	20 wt % - 5g	10 wt% - 2.5g
25g UHTR	0.01 wt% - 0.025g	15 wt% - 3.75g	15 wt% - 3.75g
25g UHTR	0.01 wt% - 0.025g	25 wt% - 6.25g	5 wt% - 1.25g

Table 5 - Results from Experiment 2

15wt% MCF/15wt% PMB		
Time	Temperature	Viscosity
5	25	Extrudable
10	25	Extrudable
15	25	Extrudable
20	24	Extrudable
25	24	Extrudable
30	23	Not-Extrudable

This experiment was not able to be completed and results were only produced for 15wt% MCF and 15wt% PMB. The intention was to test 3 different loading levels of fillers, all three being a total of 30wt%. The results for 15wt% MCF and 15wt% PMB can be observed in table 5. Even though the experiment didn't go as planned, observations from it were used to adjust the next experiments loading levels.

Experiment 3 – Workable Life with Fillers

Experiment 3 followed the same procedure as experiment 2 but adjustments were made to the loading levels of the fillers. The loading levels and experimental setup can be observed in table 6.

Table 6 - Experimental Set Up for Experiment 3

Resin	Catalyst	MCF	PMB
40g UHTR	0.1 wt% - 0.04g	20 wt% - 8g	10 wt% - 4g
40g UHTR	0.1 wt% - 0.04g	15 wt% - 6g	15 wt% - 6g
40g UHTR	0.1 wt% - 0.04g	10 wt% - 4g	20 wt% - 8g

The UHTR mixtures were extruded onto carboard panels labeled with different time intervals as seen in figure 10. This allowed for observation of how the resin slurry acted. The dimensional stability of the 10/20 mixture was good from start to finish but the mixture had the shortest workable life. The 15/15 mixture had decent dimensional stability after 15 minutes but had a slightly shorter workable life than 20/10. Dimensional stability is an important consideration when developing materials for 3D printing because layers need to adhere to each other without sinking into one another.

Figure 10 - Extruded Mixtures on Cardboard

The 20wt% MCF and 10wt% PMB had the longest "extrudable" life at 45 minutes. This loading level was selected to use in later experiments.

Observations

Upon completion of these experiments it was concluded that a catalyst ratio of 100:0.1 was too small to have a significant effect on the resin and it was also very

challenging to measure consistently with the equipment available. This was determined by putting catalyzed specimens in the oven under the cure cycle recommended on UHTR's PDS, they didn't have dimensional stability. It was also concluded that 30wt% is too high of a loading level and should be lowered to 20wt% or below. These observations led to a reevaluation of the research. Backtracking was necessary to better understand UHTR on its own, as multiple inconsistencies with resin batches were observed.

Later Experimentation

At this point in the research, observations from the initial research were evaluated. This led to a change in scope for this project and a redefinition of the deliverables for the research. It was decided to test the feasibility of UV curing UHTR, study the removal of IPA from UHTR and compare the effects of the 3 selected catalysts. During this time, inconsistencies in UHTR became more prevalent and decisions were made to use UHTR-F, the solid resin, to overcome manufacturer quality issues.

Pellet Manufacturing

After discussions with Jarrod Buffy from Techneglas, LLC, the idea of creating UHTR composite pellets was recommended. The purpose of this experiment was to make UHTR pellets that could be melted and extruded, which would eliminate the need to have mixing in the 3D printing process, simplifying it. It would also show if a UHTR composite can melt after introducing the catalyst. The pellets would already have the fillers mixed in so they would be ready for extrusion immediately. For this experiment, UHTR-IPA was degassed to remove as much IPA as possible. The resulting UHTR had

3-5% IPA, this number was based on weighing the resin before and after degassing. The UHTR was melted at 80°C in a water bath and fillers were mixed in at 20wt% MCF and 10wt% PMB. Two mixtures were created, one with a catalyst (Geniosil GF 91) and one without the catalyst and they were put in the refrigerator to solidify. The next day they were pulled out and heated to test if they would melt with the fillers. The mixture with the catalyst did not melt but the one without catalyst did although it didn't flow well at all. Based on the results, this idea was abandoned, and no further tests were done.

Figure 11 - UHTR Composite "Pellets"

UV Curing

During discussions with Techneglas's polymer chemist, it was suggested that UHTR has a chemical formulation that may support UV curing. The feasibility of UV curing the UHTR-IPA resin was tested at 6 different energy densities using a Spectroline Model BIB-150P Ultraviolent Lamp (365nm) with an intensity of 4,500 µW/cm2 at 15 inches (38cm). The lamp was attached to an off the shelf work light stand with zip ties and raised 15 inches above UHTR in a glass beaker.

Figure 12 - UV Curing Testing Equipment

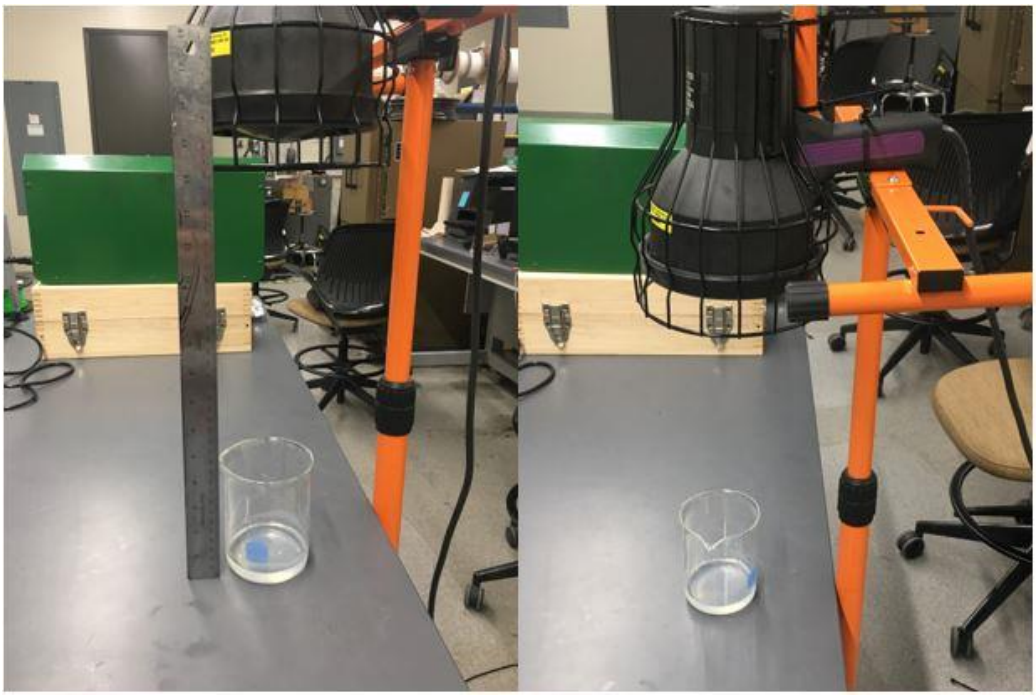

Figure 13 - UV Curing Experimental Set Up

Energy density and power density are the two most important parameters to consider when UV curing a resin. Energy density is the energy per surface area, usually measured in joules or millijoules per square centimeter. To cure a UV curable resin, it must be supplied enough energy to activate the photo initiators within the resin. The energy requirement is dependent on many variables including photo initiator concentration, amount of material, chemical makeup and cure thickness (Gotro, 2016). Power density is the intensity or rate at which UV light is supplied to the resin. Power density is power per surface area and is measured in watts or milliwatts per square centimeter. Power density and peak irradiance are often interchangeable but there is a significant difference. Peak irradiance is the highest power density supplied to a UV curable resin, while power density is the average irradiance supplied to a UV curable resin.

$$Power * Time = Energy$$

$$Peak\ Irradiance * Exposure\ Time = Energy\ Density$$

$$Watts * Time = Joules$$

$$\frac{mW}{cm^2} * seconds = \frac{mJ}{cm^2}$$

Figure 14 - UV Curing Equations (Gotro, 2016)

Figure 14 above shows the equation used to determine the time of exposure needed for a 4,500 µW/cm2 UV lamp to achieve 6 different energy densities. After converting the intensity of the lamp to mW/cm2, the energy densities were easily calculated. Table 7 below shows the energy densities tested, time of exposure and observations about the UHTR resin at each energy density. The energy densities were selected based off a paper by Joe Bennett studying the curing mechanisms of photopolymers used in 3D printing processes (Bennett, 2017). The energy densities stayed below 1000 mJ/cm2. The time of exposure was also considered when determining energy densities to test, and this led to the highest energy density value being 5000 mJ/cm2 at around 18.5 minutes using 4.5 mW/cm2 of irradiance. It should be noted that time of exposure can be manipulated by changing the intensity of the radiation source.

Table 7 - UV Curing Test Observations

Energy Density (mJ/cm2)	Exposure Time (sec)	UHTR Observations
100	22.22	No Change
500	111.11	No Change
1000	222.22	No Change
1500	333.33	No Change
2000	444.44	No Change
5000	1111.11	No Change

At the conclusion of the 6 tests, UV light showed no noticeable effect on the UHTR resin at the 6 different energy densities. The results led to the conclusion that the resin is not UV curable without a change in formulation.

Catalyst Characterization

The goal of these tests was to understand the time frame for the extrusion process of a UHTR-IPA mixture after crosslinking had been initiated with a catalyst. The potential additive manufacturing process could utilize a long or short workable life, so it is important to understand the different time frames available for each catalyst at varying weight percentages. It was recommended not to exceed 10wt% catalyst by the UHTR manufacturer. The starting wt% for catalyst 1 and 3 were selected using the manufacturer recommendation on UHTR's PDS and further percentages were selected based on observation. Catalyst 2 was started at 2wt% because it was similar to the other two catalyst's starting points. The tables below show the workable life of the resin after the 3 catalyst were added.

Table 8 - Catalyst 1 (Geniosil GF 91)

Catalyst wt%	Workable Life in Minutes
2	45
4	25
5	19
10	23

Table 9 - Catalyst 2 (BIS(3-TRIETHOXYSILYLPROPYL)AMINE 95%)

Catalyst wt%	Workable Life in Minutes
2	60+
4	30

Table 10 - Catalyst 3 (Titanium (IV) Butoxide)

Catalyst wt%	Workable Life in Minutes
3	90
4	40
5	17
7	10

Observations

Catalyst 1 had the most consistent results and linearity when increasing/decreasing catalyst wt% until it got up to 10. The cured specimens for catalyst 1 were observed to be significantly brittle, more so than the other specimens using different catalysts. Catalyst 2 was observed to have a drastic decrease in workable life from 2 to 4wt%. These samples were observed to be more ductile than the others. Catalyst 2 needs further characterization to determine its overall workable life range. Catalyst 3 shows a major jump in workable life from 3 to 4wt% and the workable life decreased around 50% for each increase in wt%. These tests were all ran using the same batch of UHTR-IPA and when it ran out, the next batch was observed to be a much different viscosity and yielded different results for the same catalyst ratios. That is why further tests were not completed. This was another sign that UHTR-IPA had quality issues and at this time, different batches could not provide consistent results. This led to a change in approach which is discussed in more detail later.

IPA Removal

The degassing chamber in the Advanced Composites Lab at Texas State University was used to remove the IPA from UHTR. This particular degasser uses a 6-cfm vacuum pump. The UHTR-IPA was degassed for 2.5 hours and removed in 15-minute intervals to measure the weight. For ease of calculation, 100 grams of UHTR (35

grams of IPA) was used for each experiment. The weight of the IPA was calculated based on the weight of the UHTR left in the beaker. Three tests were done at room temperature and the average of the results is shown in figure 15. After 2.5 hours, less than 4 grams of IPA remained from the initial 35 grams.

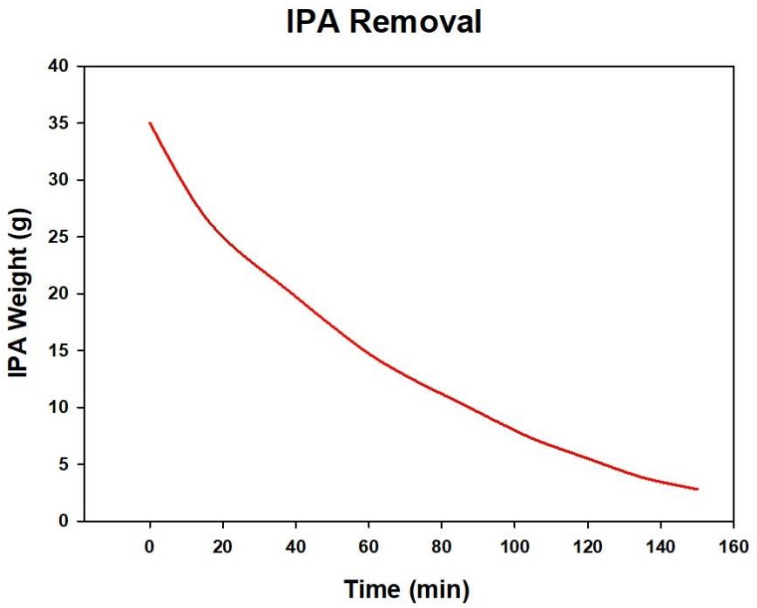

Figure 15 - IPA Removal Average Results

Observations

After 2.5 hours, less than 4% of IPA was left in the UHTR. The rate of removal was dictated by the vacuum pump and the IPA could likely be removed more quickly with a larger pump. The addition of heat might help the removal process as well. Removing 100% of the IPA content in UHTR would likely be a more daunting task, as the IPA is removed the more viscous the resin becomes, creating a harder path for the IPA to evaporate.

Adding IPA to UHTR-F

After receiving 3+ batches of UHTR from Techneglas, LLC., there was a noticeable difference in viscosity with each batch. To ensure consistency, IPA was added to the UHTR-F (all solids) in the ACL at Texas State University. UHTR-F melts at around 80°C but is still too viscous to extrude from a 3D printer, especially if the 80°C temperature isn't maintained. To counteract this, IPA was added to improve UHTR-F's ability to print. To accomplish this task the proper wt% of IPA was found and the most efficient way to dissolve UHTR into IPA was explored.

Dissolving UHTR-F into IPA

Considering the resources available in the ACL, 4 methods were used to dissolve UHTR-F into IPA. All tests were done using 85 grams of UHTR-F and 15 grams of IPA to prove the best mixing process. Later, different loading levels of IPA would be tested to find the optimal wt% for 3D printing.

The first method consisted of using a hot plate at 80°C and mixing together the two materials with a glass stir in a beaker. The UHTR-F was crushed into a fine powder with the idea that it would dissolve faster than large chunks. The first attempt of this method used a beaker with IPA on the hot plate at temperature while the fine UHTR-F powder was poured in incrementally and stirred.

For the second attempt, the UHTR-F powder was placed in an oven at temperature and when it was melted it was immediately placed on the hot plate at temperature, where the IPA was poured in and mixed by hand.

The third attempt used a Breville mixer to mix the UHTR-F powder into IPA, that had been previously placed in the mixing bowl, at room temperature. This method was the slowest of the 4 and is likely better suited for large batches. Due to the cost of the resin, only small batches will be tested so no resin will go to waste.

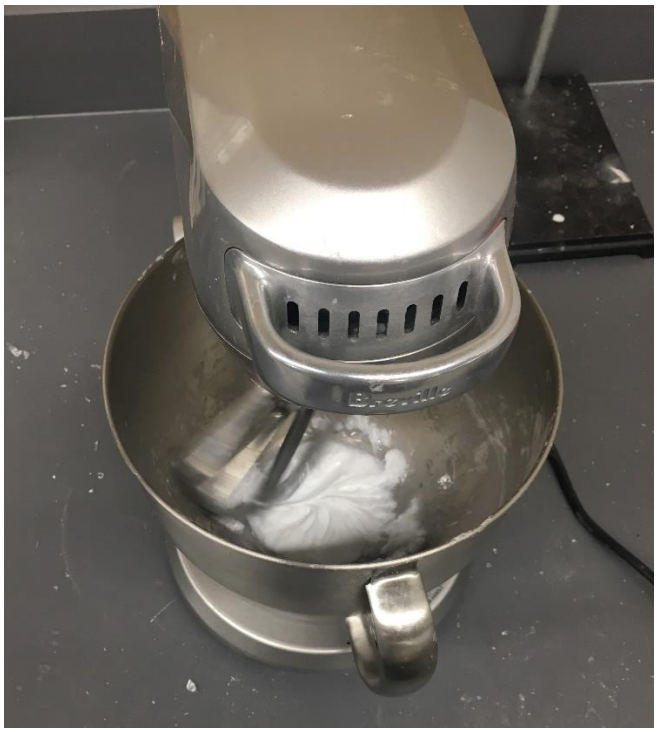

Figure 16 - Breville Mixer

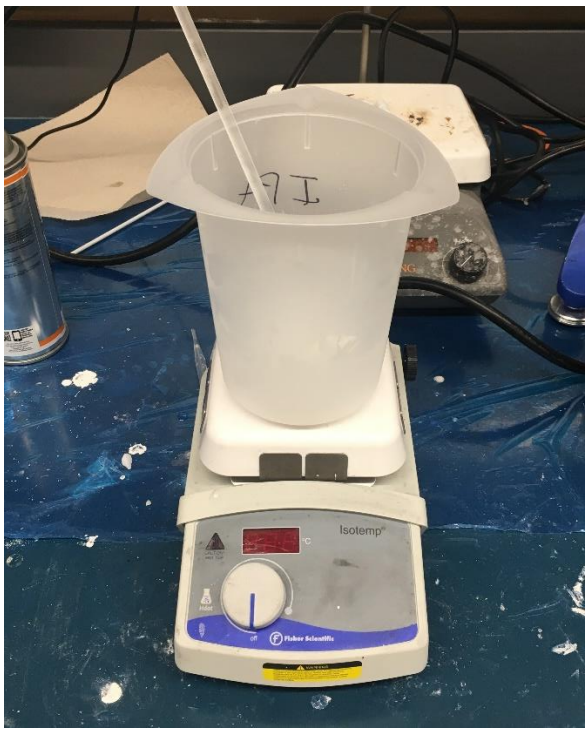

Figure 17 - Hot Plate

The last method was simple, UHTR-F powder was mixed into IPA by hand at room temperature. This attempt did effectively dissolve the UHTR-F into the IPA but heat obviously speeds the process up. The only benefit to this method was that there was less chance of IPA evaporating than when using heat.

The hotplate and oven method were chosen to as the best option for further mixing of UHTR-F and IPA. It was later observed that melting the resin at 100°C provided a better mixing viscosity. This method created a uniform mixture that can be observed in figure 18. Breaking the solid chunks into a fine powder also proved useful, as the bigger chunks took much longer to dissolve. The Breville mixer eventually created a uniform mixture but it was “whipped” as seen in figure 19, likely due to air being deposited into the resin during

mixing. The hot plate/oven method was moved forward with to create samples for rheology characterization.

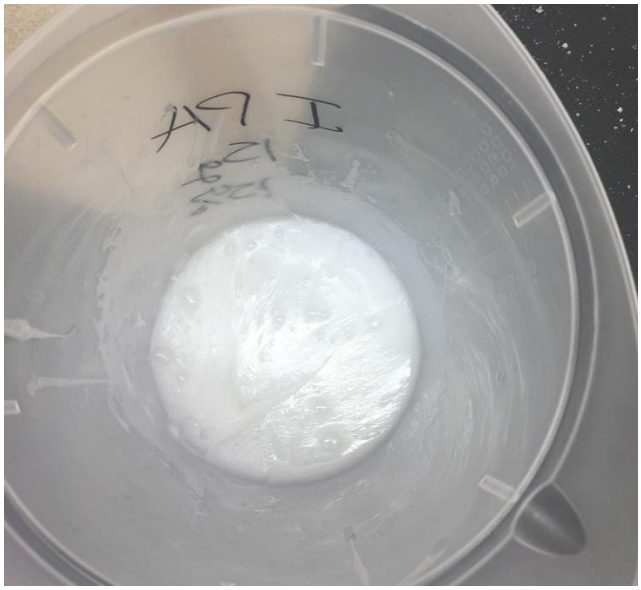

Figure 18 - Hot Plate/Oven UHTR-F/IPA Mixture

Figure 19 - "Whipped" UHTR-F/IPA Mixture

III. CHARACTERIZATION

Dynamic Mechanical Analysis (DMA)

DMA coupons were fabricated using a mold manufactured from silicone and a 3D printed mold positive. The coupons were prepared to the specifications of the single cantilever beam test and the tests were performed at TRI-Austin on their TA Instruments DMA Q800. Three coupons consisting of UHTR-F resin mixed with 3wt% of one of Titanium (IV) Butoxide, Bis(3-Triethoxysilylpropyl)amine 95%, Geniosil GF 91 and one consisted of UHTR-F with 10wt% MCF/5wt% PMB and 3wt% Geniosil GF 91. To manufacture the coupons, UHTR-F was melted in an oven and the catalyst was immediately mixed in. After the catalyst was thoroughly mixed by hand, the mixture was placed into the mold using tongue depressors and uniformly distributed. The goal for the DMA tests was to understand how each catalyst is affecting the resin and which one is providing the best dimensional stability through storage modulus loss.

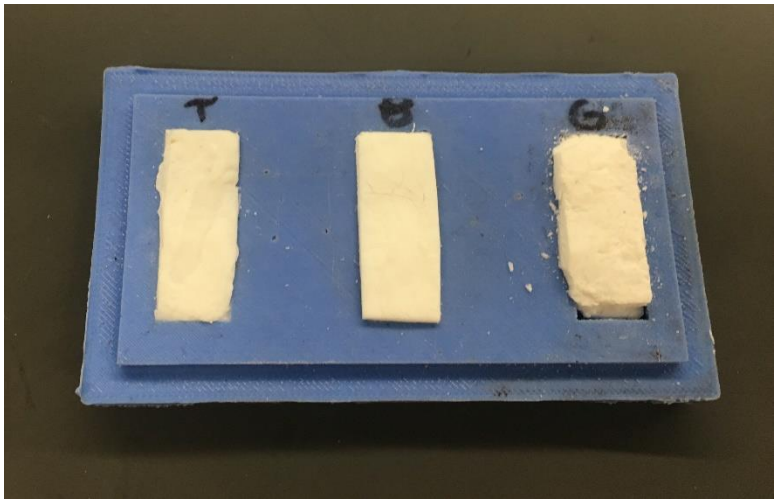

Figure 20 - DMA Coupons in the Mold

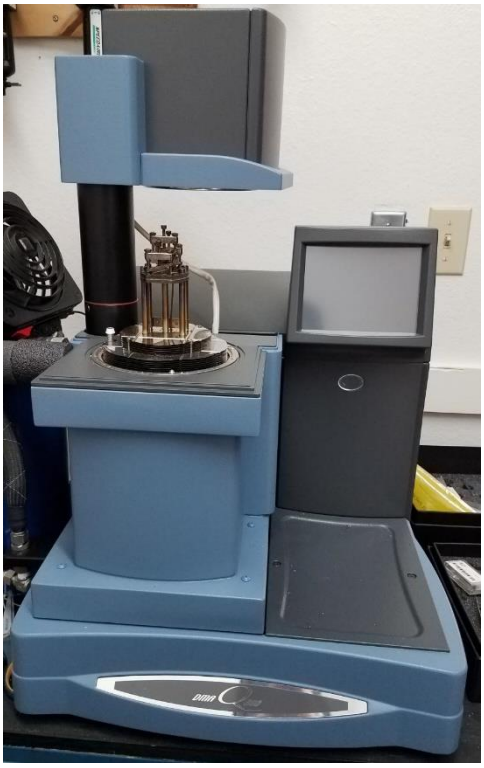

Figure 21 - TA Instruments DMA Q800

The specimens were put in the oven at 80°C to test if they would melt after introducing the catalyst, this is important because the resin would be difficult to clean out of the intricacies of the machine and if they melt, they haven't started crosslinking. After three different coupons of Titanium (IV) Butoxide melted in the oven, it was decided not to move forward with the catalyst. This was an interesting observation because it is recommended by the manufacturer. Higher weight percentages also failed the melting test.

Figure 22 - Melted Titanium (IV) Butoxide DMA Specimens

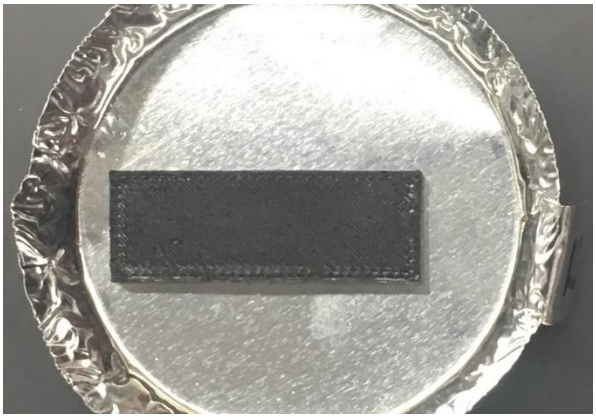

Figure 23 - UHTR 10% MCF/5% PMB DMA Coupon

Rheology

IPA Viscosity

It was concluded from previous experiments that IPA was necessary to keep UHTR with the addition of fillers at a viscosity that can be extruded. To determine the appropriate amount of IPA needed to reach a workable viscosity, rheological analysis was done using a Haake Viscotester iQ rheometer in the Micro Systems & Manufacturing Lab at Texas State University. UHTR-IPA is manufactured with 35wt% IPA, so using

that as the baseline, three different UHTR-IPA mixtures were manufactured using the techniques described in previous sections. Initially, 5wt%, 10wt% and 15wt% IPA were to be tested but 5wt% was observed to be much too viscous and was replaced with 20wt%. The IPA was observed to cause porosity in the cured resin, so the goal was to use the lowest wt% of IPA possible without compromising extrudability.

Figure 24 - Haake Viscotester iQ Rheometer

After the UHTR test samples were manufactured, the mixtures were placed in 60mL catheter tip syringes so that they could be placed in the rheometer. The Haake Viscotester iQ requires 3mL of material to run a test and the volume markings on the

syringes were used to ensure an accurate amount of material was dispensed. The figure below shows the UHTR-IPA mixture before and after the plate is lowered onto the sample in the rheometer.

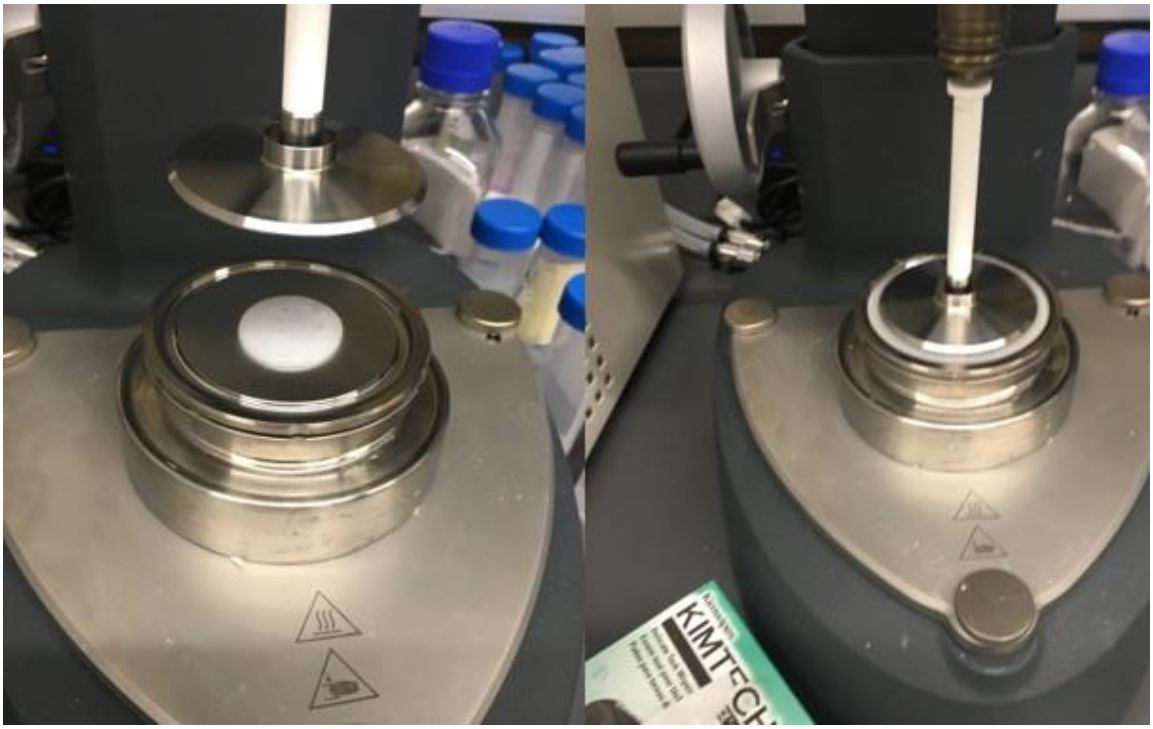

Figure 25 - Plate Being Lowered onto UHTR Test Specimen

Filler Viscosity

After determining the proper level of IPA to use with UHTR, different loading levels of the fillers were added to the new UHTR-IPA mixture to understand their effects on viscosity. In the initial experimentation, a total of 30wt% fillers were mixed into UHTR and tested. Such a high amount caused the mixture to be extremely viscous and unable to extrude effectively. For this rheology study, the fillers were added at smaller loading levels and three mixtures were manufactured for testing. Two of the three mixtures had a total of 15wt% fillers while the other had a total of 20wt%. The resin systems that were tested are shown in table 11. All tests used a total of 50g of material.

Table 9 - Filler Rheology Specimens

UHTR (g)	MCF wt%	MCF (g)	PMB wt%	PMB (g)	Total wt%
40	10	5	10	5	20
42.5	10	5	5	2.5	15
42.5	5	2.5	10	5	15

The test specimens were manufactured using methods outlined in previous sections but with the addition of the fillers. The fillers were added in small increments after the UHTR was dissolved into the IPA. After the fillers were thoroughly mixed into the UHTR, the mixtures were placed into 60ml catheter tip syringes, following the same procedures as the previous rheology tests. During this process, it was observed that a total of 20wt% was too viscous for testing and the 20wt% test was abandoned, leaving two tests to be performed.

Figure 26 - 10wt% MCF/5wt% PMB Rheology Test

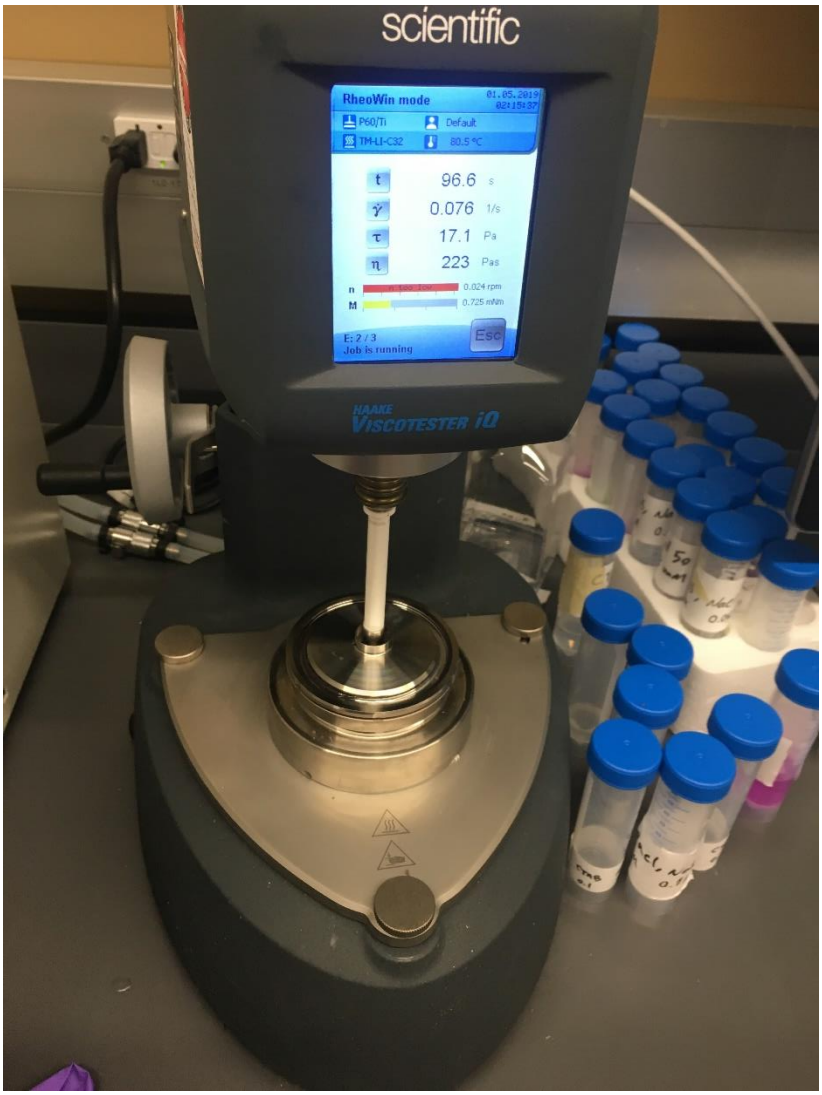

Figure 27 - 5wt% MCF/10wt% PMB Rheology Test

Thermogravimetric Analysis (TGA)

TGA was used to characterize the mass loss of the UHTR composite specimens. The analysis was done on a TA Instruments SDT 650 machine in the ACL at Texas State which is capable of simultaneous thermal characterization methods, differential scanning calorimetry (DSC), and thermogravimetric analysis (TGA). The machine is pictured below in figure 28.

Figure 28 - TA Instruments SDT 650

The machine requires 10mg of material in no particular shape to complete a test. The UHTR specimens were prepared by hand in a 50mL beaker because only a small quantity was required. The specimens are shown in figures 29-31 below. A total of 6 tests were ran, 1 for each of the following specimens:

- UHTR-F – 3% Catalyst 1
- UHTR-F – 3% Catalyst 2
- UHTR-F 10% MCF/5% PMB – 3% Catalyst 1
- UHTR-F 10% MCF/5% PMB – 3% Catalyst 2
- UHTR-F 5% MCF/10% PMB – 3% Catalyst 1
- UHTR-F 5% MCF/10% PMB – 3% Catalyst 2

All specimens used UHTR-F with 15% IPA and heated to a maximum temperature of 1500°C. The first two tests were done without fillers to study the effects of the two catalysts on the UHTR-F 15% IPA and the later tests involved varying loading levels of fillers with the two catalysts.

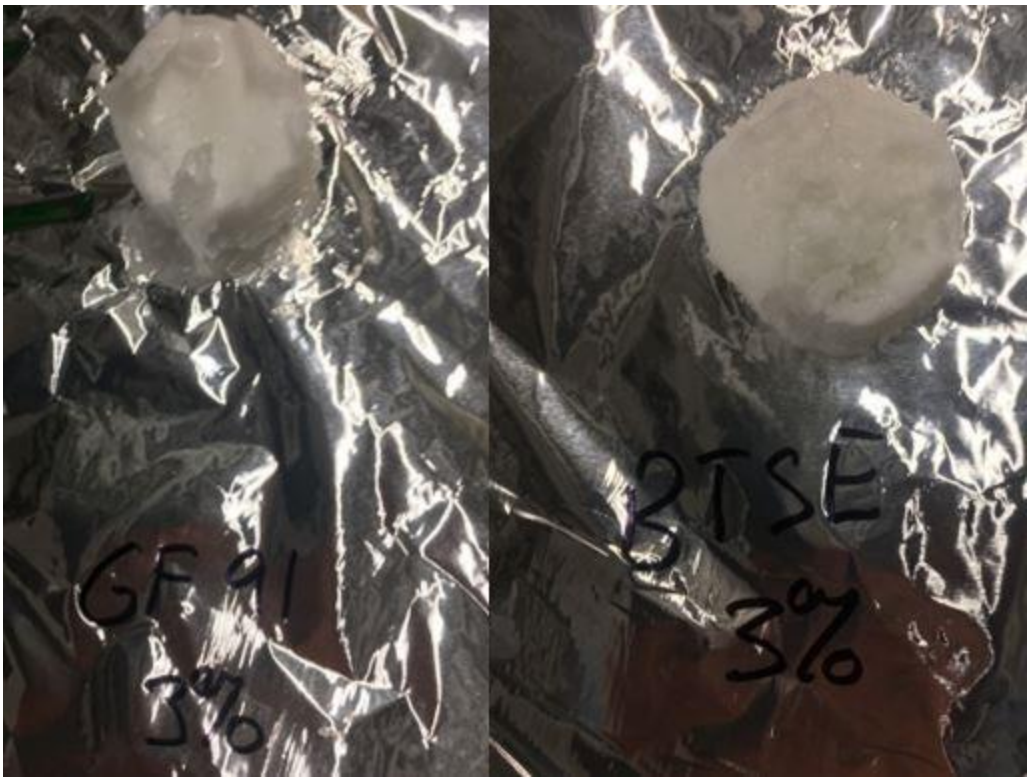

Figure 29 - TGA Specimens with No Fillers

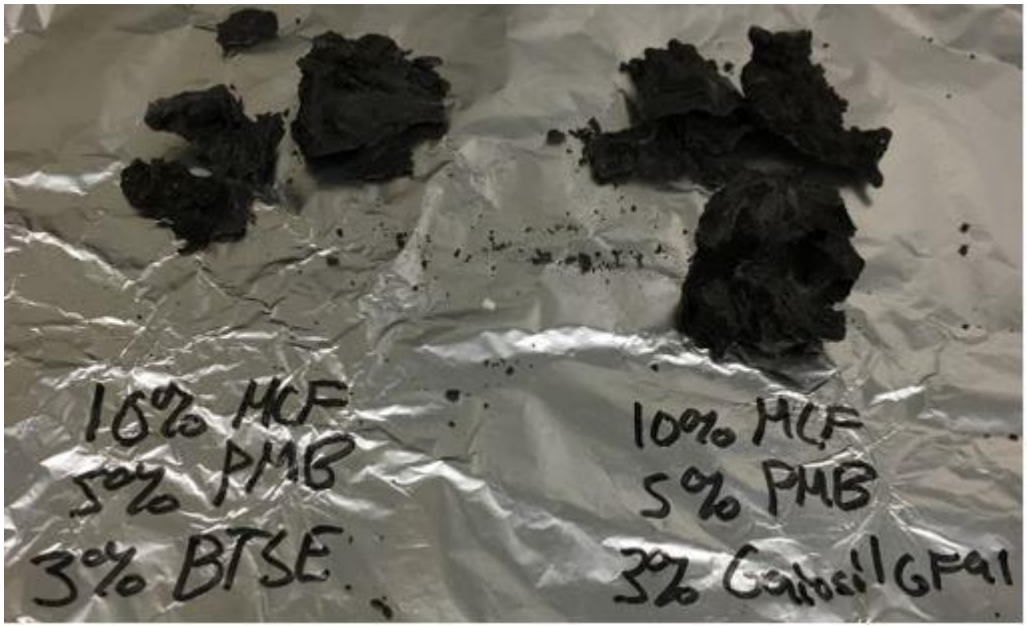

Figure 30 - TGA Specimens with 10% MCF/5% PMB

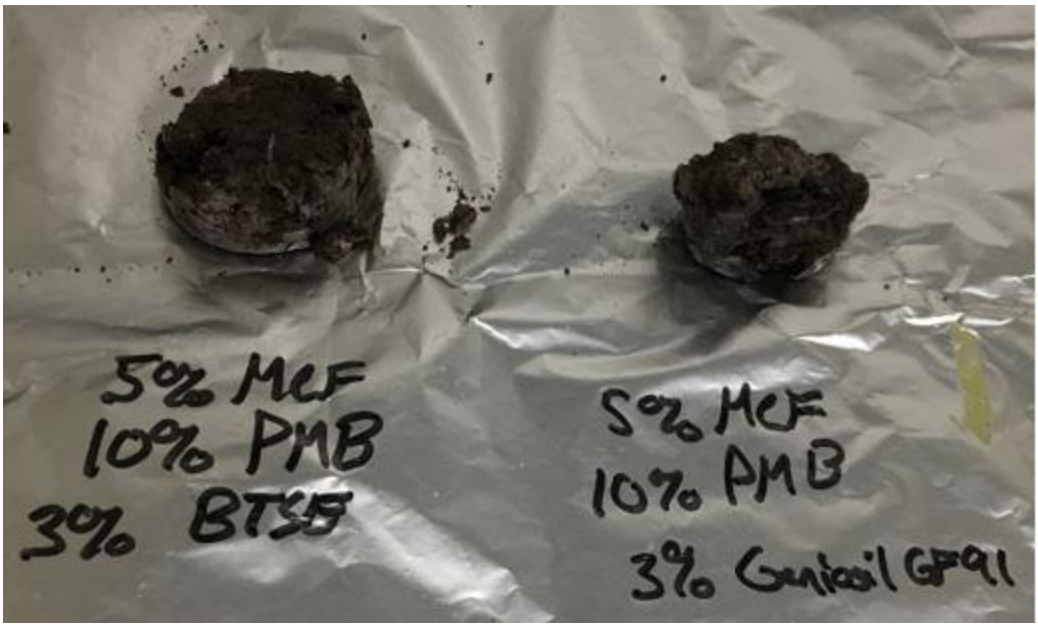

Figure 31 - TGA Specimens with 5% MCF/10% PMB

Flexure Testing

To characterize the effects of the reinforcements (fillers), flexure testing specimens were manufactured. It is important that the UHTR composite can be 3D printed but it is just as important that it can withstand aerodynamic and mechanical forces present in a realistic environment. The specimens were manufactured and tested according to ASTM D790 - 17. Two sets of specimens were manufactured using a silicon mold, a set with UHTR-F 15% IPA and 3% catalyst 1 and a set with fillers. The UHTR-F 15% IPA was loaded with 10% MCF/5% PMB after comparing the results from the previous experiments and tests. This loading level yields a workable viscosity, good thermal properties and utilizes more reinforcement. These specimens also used 3% catalyst 1.

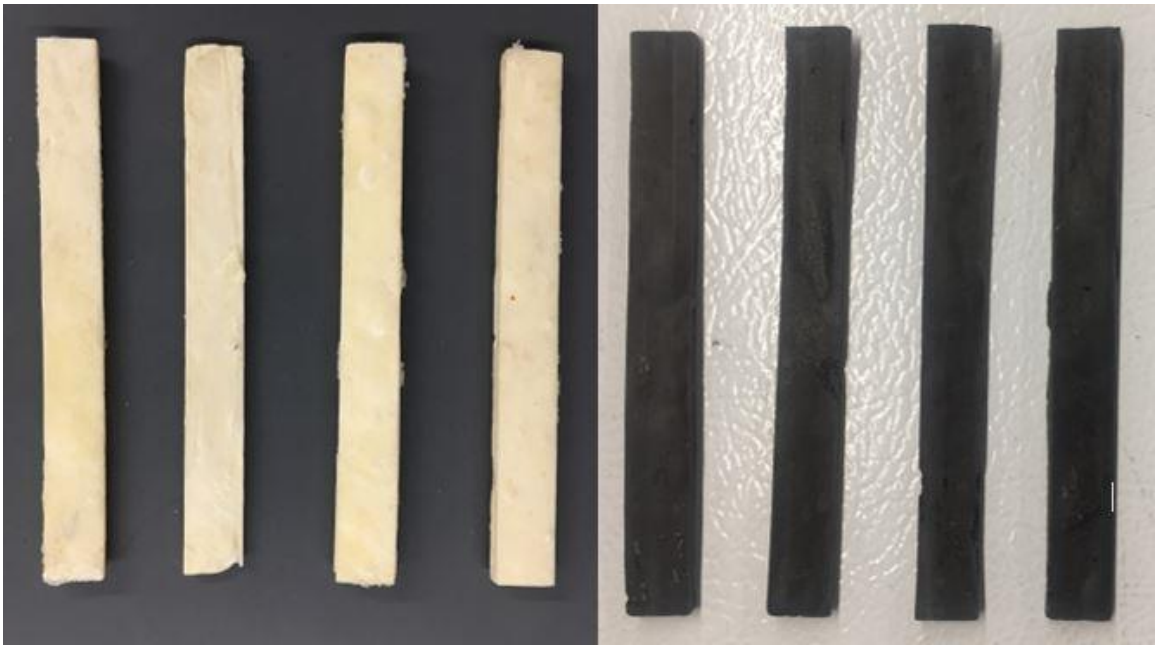

Figure 32 - UHTR Flexure Specimens, neat (left), with Fillers (right)

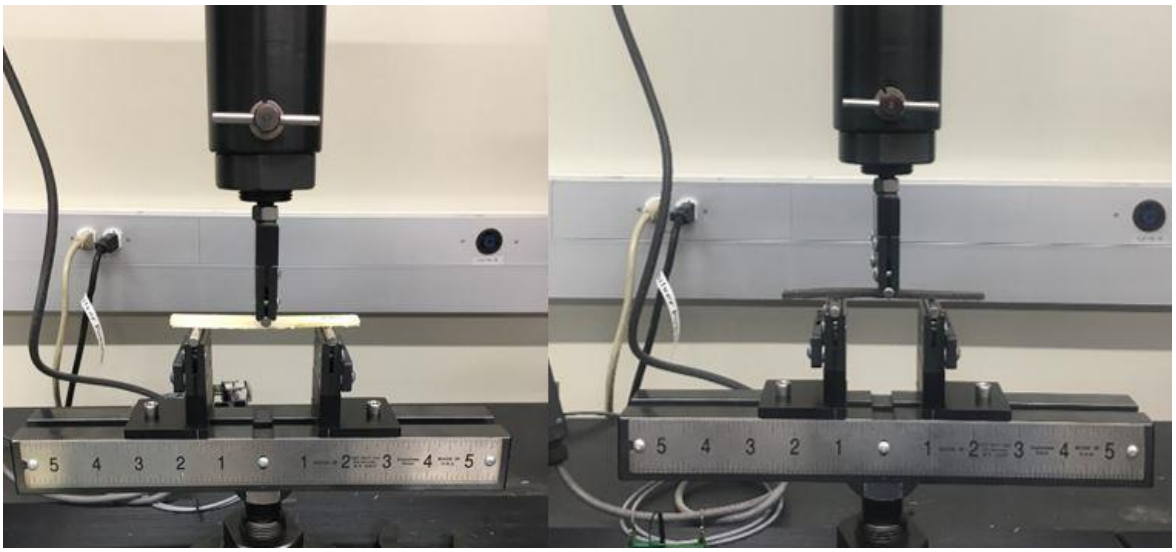

Figure 33 - Flexure Coupons in Testing Apparatus

IV. RESULTS AND DISCUSSION

Dynamic Mechanical Analysis (DMA)

DMA was performed using a TA Instruments DMA Q800 machine in the characterization lab at Texas Research Institute - Austin to understand the effects of the catalysts on the UHTR resin. Three specimens were prepared for single cantilever DMA testing. The specimens were heated at a rate of 10°C/min to a max temperature of 350°C. The physical state of the coupons after heating can be observed in figure 34, Bis(3-Triethoxysilylpropyl)amine 95% on the left and, Geniosil GF 91 on the right.

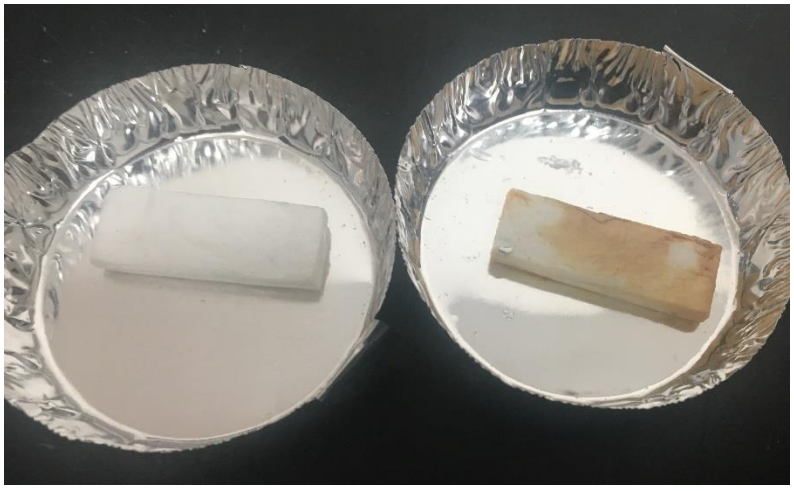

Figure 34 - DMA Coupons Post Testing

The DMA results for Bis(3-Triethoxysilylpropyl)amine 95% are shown in figure 35.

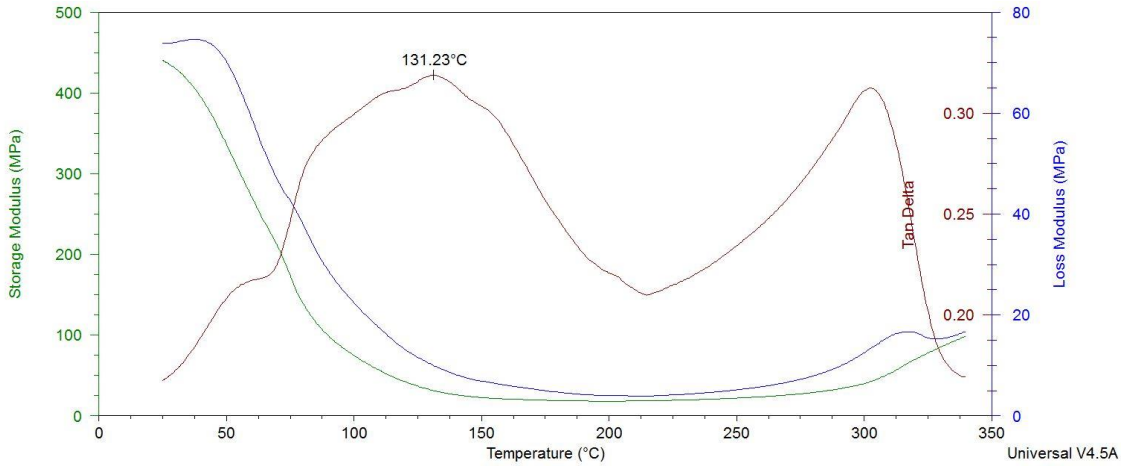

Figure 35 - DMA Results for Catalyst 2

The DMA results for N-(2-Aminoethyl)-3-aminopropyltrimethoxysilane are shown in figure 36.

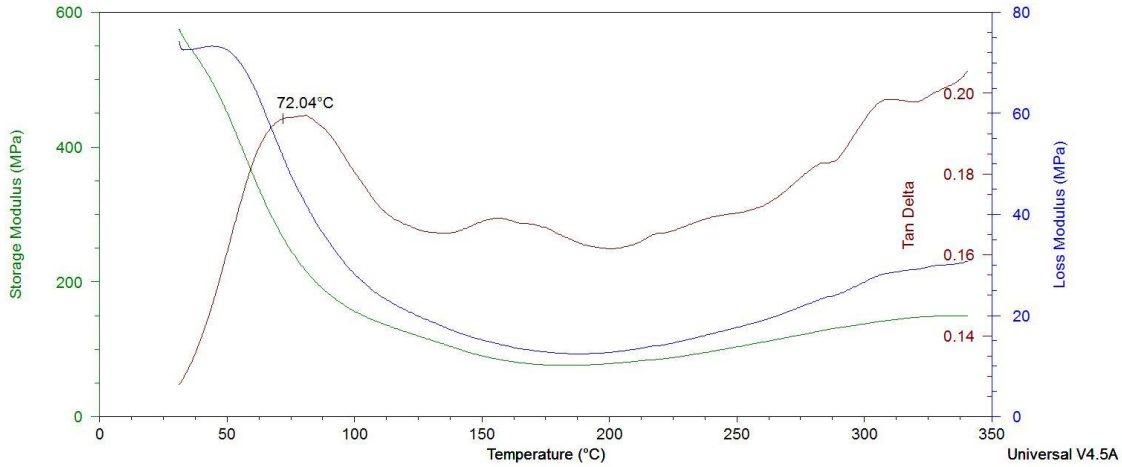

Figure 36 - DMA Results for Catalyst 1

The effects of the catalyst on the storage modulus are shown in figure 37 below. Catalyst 1 had comparatively less storage modulus loss. This was interpreted as better dimensional stability when introduced to heat. Both test specimens softened to a point and neither melted but for the purposes of this research, catalyst 1 showed better performance.

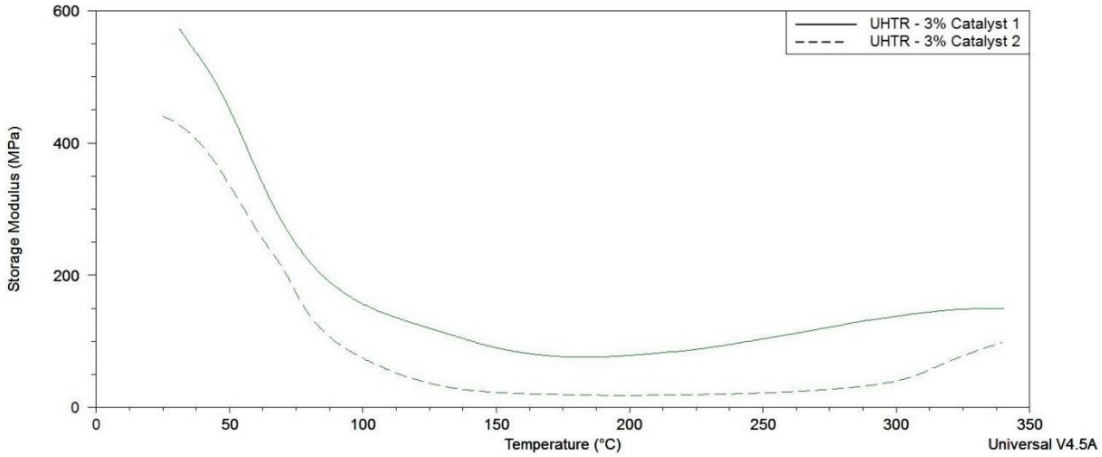

Figure 37 - Storage Modulus Comparison of the Two Catalysts

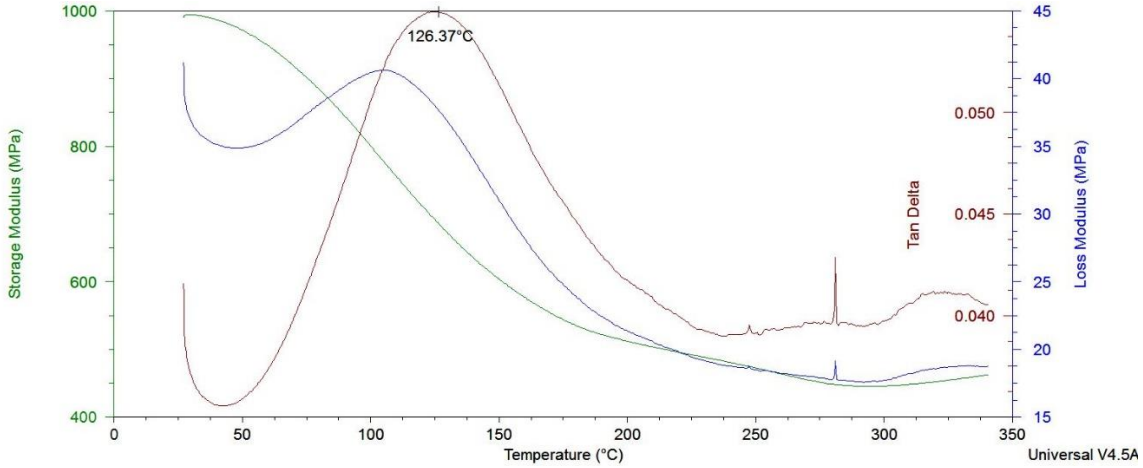

Figure 38 - DMA Results for UHTR with 10% MCF/5% PMB and 3% Catalyst 1

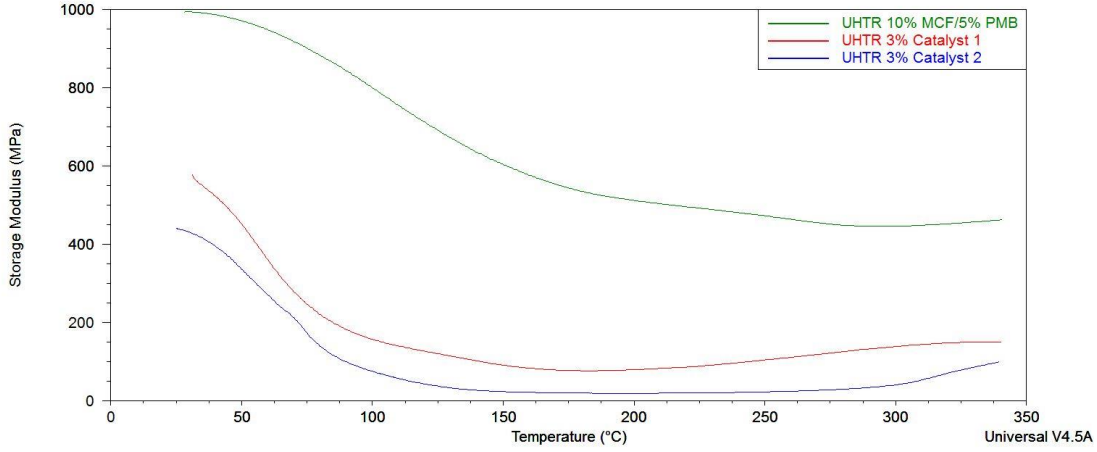

Figure 39 - Storage Modulus Comparison of the Three DMA Specimens

The addition of the fillers significantly increased the storage modulus and it can be seen in figure 39 that the fillers contribute to the dimensional stability of UHTR under thermal loads. The specimen with catalyst 2 has a higher peak tan delta, interpreted as glass transition temperature (T_g), than the other two samples, and has two significant peaks. Catalyst 1 has a significantly lower T_g than the specimen with catalyst 1 + fillers, showing another effect the fillers can have on the resin.

It is important that the UHTR composite developed in this research be dimensionally stable at high temperatures because it will need to maintain its geometry when thermally cured. If a part was printed with the UHTR composite without a catalyst, the part would melt during the thermal curing process. The purpose of the catalyst is to initiate enough crosslinking in a 3D printed UHTR composite part so that it will be dimensionally stable during thermal curing.

Rheology

The viscosity of the UHTR composite is the most important parameter to consider for 3D printing. If the composite is too viscous, it will not extrude well or possibly not at all. If the composite is lacking in viscosity, it will not maintain dimensional stability immediately after printing and run. IPA plays an important role in the material system because it decreases the viscosity of UHTR-F composite, which is solid at room temperature, enough to be extrudable at a temperature of 80°C. Rheology tests were done on UHTR-20% IPA, UHTR-15% IPA, and UHTR-10% IPA using a Haake Viscotester iQ rheometer at a temperature of 80°C. Initially, UHTR-5% IPA was to be tested but was eliminated because it was visibly too viscous to work with. Figure 40 displays the results of the shear viscosities of the different mixtures of UHTR-IPA at varying shear rates.

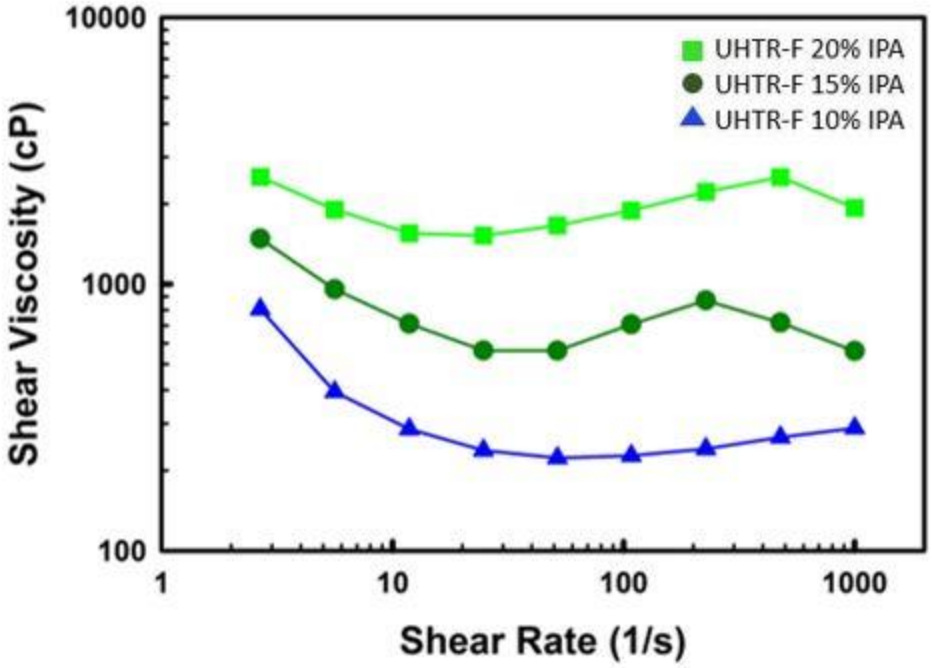

Figure 40 - IPA Viscosity Results

The purpose of this test was to find the lowest loading level of IPA that can be used in UHTR while still maintaining a reasonable viscosity for extrusion. UHTR-20% IPA was eliminated, even though it had the lowest viscosity because it had the highest loading level of IPA. Since the other two samples both yielded reasonable results, they were further tested by mixing the fillers in. The UHTR-15% IPA was observed to be workable after the addition of fillers but when fillers were added to UHTR-10% IPA, it was not reasonably workable. These results and observations were used to select the final IPA level for the material system, 15%. UHTR-15% IPA was used for all further characterization.

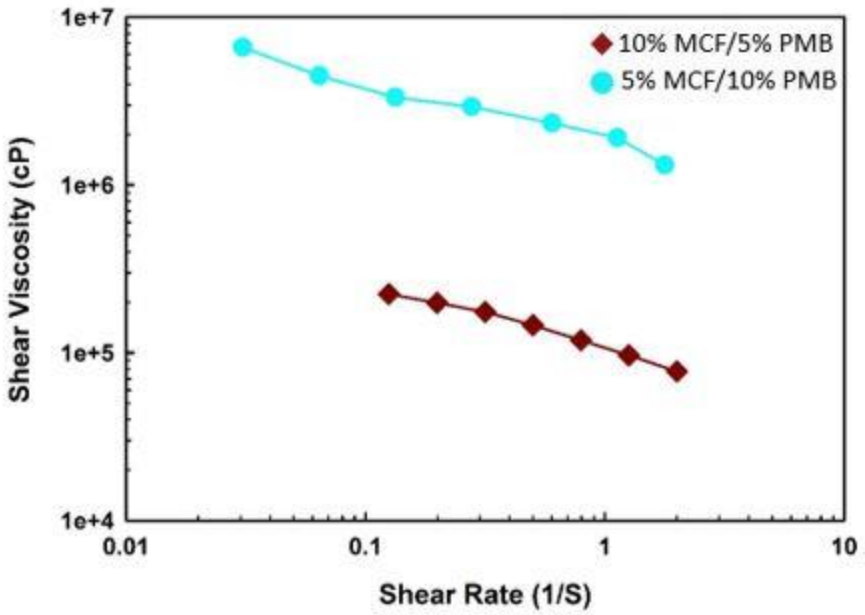

Figure 41 - Filler Viscosity Results

The material system needs to have enough viscosity to maintain dimensional stability but it cant be too viscous, as it wont be able to extrude. The results of the rheology study with fillers is shown in figure 41. The addition of fillers causes a drastic increase in viscosity which can be observed when comparing figure 40 with figure 41. At 80°C the specimen consiting of 10% MCF/5% PMB had a peak shear viscosity of 224200 cP which is comparable to peanut butter. The specimen consisting of 5% MCF/10% PMB had a peak shear viscosity of 6609000 cP which is comparable to caulk. The results clearly show that a lower loading level of microballoons will yield a more desirable viscosity. This was an expected result, as previous researchers had observed that microballoons have a considerable effect on viscosity. The specimens experienced shear thinning, which means as the shear rate increases, the UHTR composite's viscosity decreases, this is seen in non-newtonian fluids. The auger extruder puts a shear force on the resin as it extrudes and could facilitate the extrusion of more viscous material

systems. This conclusion will need to be explored further in future work. Due to its lower viscosity and higher loading of reinforcement (MCF), the 10% MCF/5% PMB was deemed the most promising candidate to move forward with but a final determination couldn't be made because the two material system needed more characterization before a final selection was made.

Thermogravimetric Analysis (TGA)

Catalyst

The results of the mass loss characterization for UHTR-F 15% IPA with catalyst 1 and 2 are shown in figure 42 below. Ramping up to a maximum temperature of 1500°C, catalyst 1 retained the most mass but catalyst 2 performed very similarly. The selection of the final material system is not based solely on one test and since both catalysts performed about the same in this test, a determination wasn't made on which to move forward with without considering all previous work.

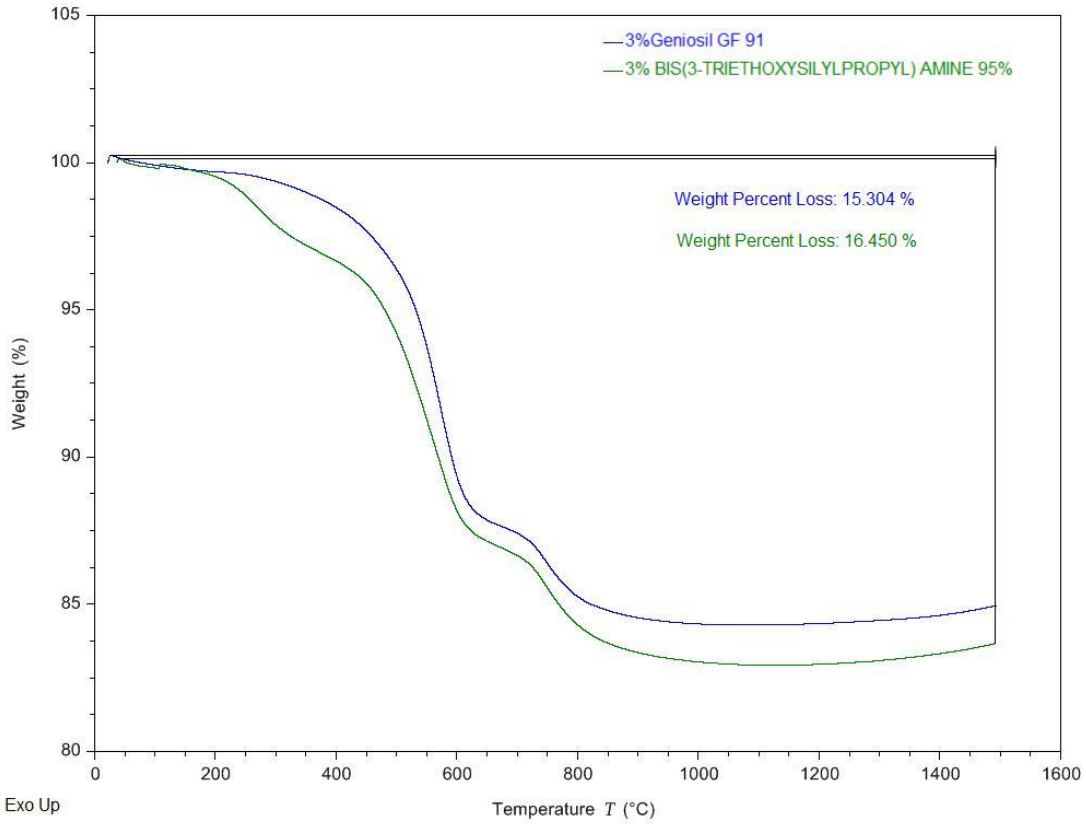

Figure 42 - Weight Loss Comparison of the Two Catalysts

Fillers

The addition of fillers also yielded very close numbers in terms of mass loss. The higher loading levels of PMBs, as expected had better TGA performance because phenolics will follow the same degradation mechanism as the UHTR and contribute to the char yield. For 5% MCF/10% PMB, catalyst 1 was slightly outperformed by catalyst 2 but not enough to say that catalyst 2 is clearly better. For 10% MCF/5% PMB, catalyst 1 outperformed catalyst 2 by almost 1.5%, which again is not significant enough to decide on which is the better choice. Previous work must be considered along with this data to determine the best catalyst for the material system.

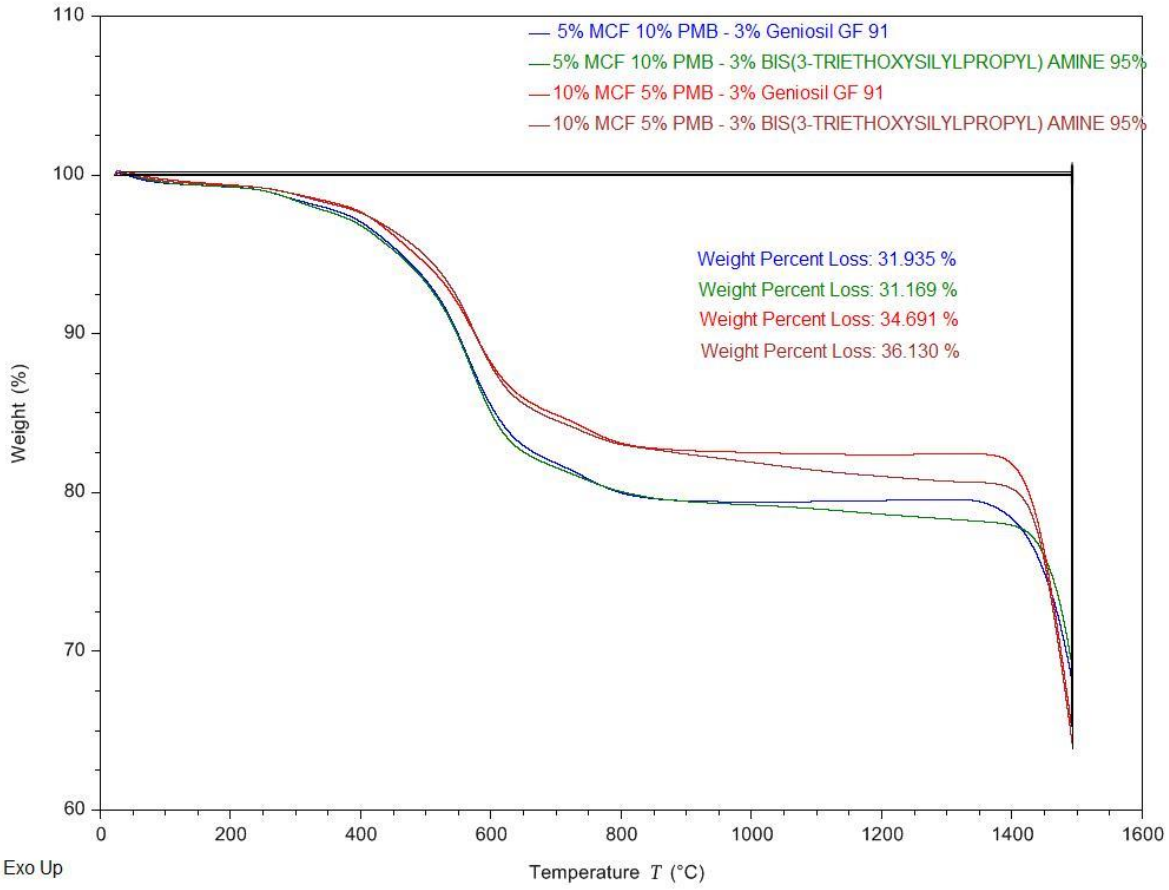

Figure 43 - Weight Loss Comparison of the UHTR Composite Specimens

Flexure Testing

Two sets of UHTR specimens were flexure tested following ASTM D790 - 17. A control set using UHTR-F 15% IPA and a set including 10wt% MCF and 5wt% PMB. Each specimen whether it had fillers or not was observed to be very brittle but there was no major porosity issue based on observation. The results of the tests can be observed in figures 44 and 45.

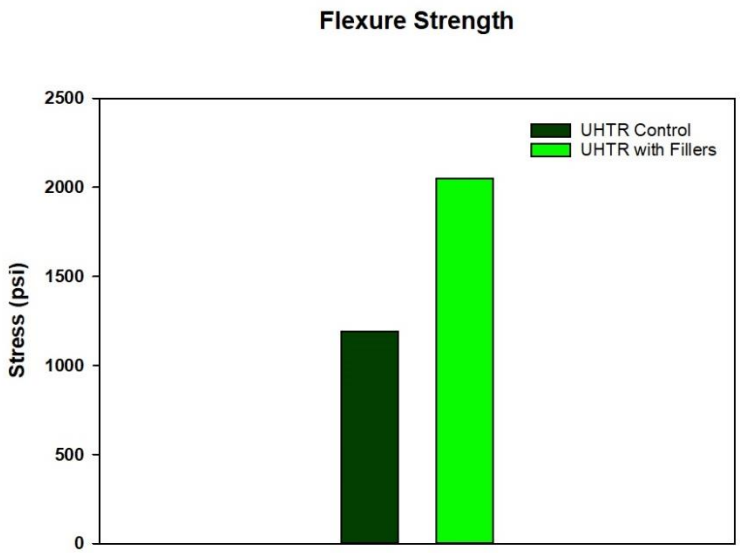

Figure 44 - Flexure Strength Comparison

The control specimens had a flexure strength of 1189.5 psi, which is much lower than common polymers. The fillers pushed the flexure strength of UHTR to 2049 psi which is still considered a low value when compared to common polymers. This does show that the fillers do affect the mechanical properties in a positive way.

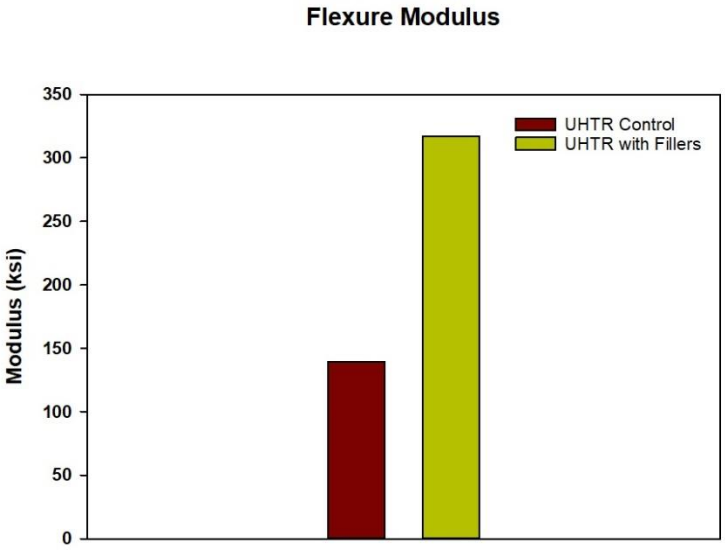

Figure 45 - Flexure Modulus Comparison

The flexure modulus had a larger increase when the fillers were added to UHTR. The control specimens had a modulus of 139.2045 ksi while the filled specimens showed an increase to 317.0528 ksi. These numbers are comparable to those of common thermoplastic polymers. Again, the fillers showed their effects by more than doubling the modulus. These numbers are promising but future work must focus on how these values can hold up against real world situations.

V. PROTOTYPE MANUFACTURING

A goal of this research is to develop a proof of concept process for 3D printing the UHTR composite in an effective manner. Although this research has focused on developing the material system, manufacturing a 3D printer capable of printing the UHTR composite is critical so that characterization specimens can be fabricated, and the material system can be fine-tuned. The two present options were to develop a new process or adapt a current process to this new application. Off the shelf clay printers are ideal for this application because their printing parameters closely match those necessary for printing a thermoset resin and most are open source machines. Figure 46 shows an example of a custom clay printer using a syringe extruder for liquid deposition modeling (LDM) that was found on Thingiverse, a website that promotes sharing of 3D printing projects. Clay printers like the WASP Delta 2040 clay printer are commercially available and ideal for this application but can be very expensive. After considering the options, it was decided that a TAZ LulzBot available in the Advanced Composites Lab at Texas State would be used as the printing platform and an auger extrusion mechanism would be developed in house at the new Makerspace in Ingram Hall.

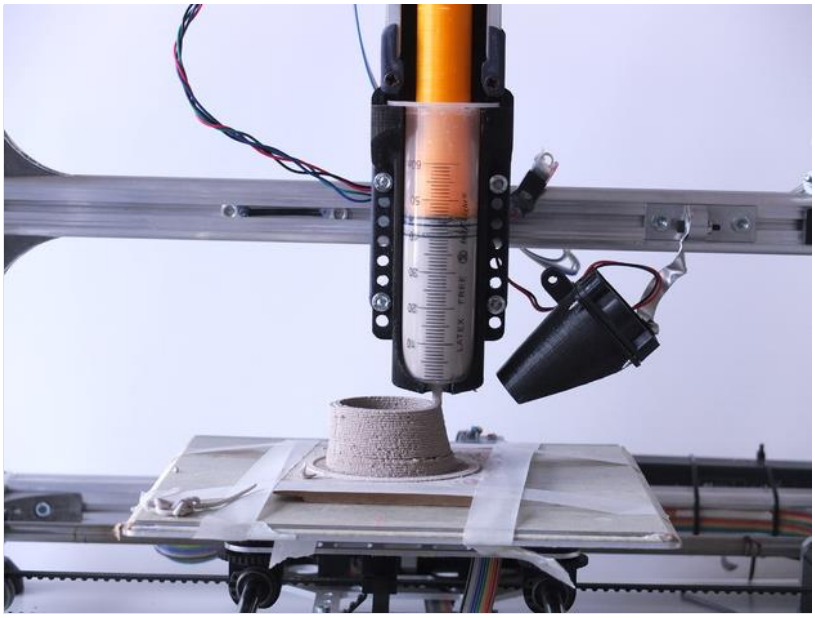

Figure 46 - 3D Printed Syringe Adapter for 3D Printers

LulzBot TAZ 5

LulzBot is an affordable 3D printer product line by Aleph Objects, Inc. and is a popular desktop printer used by hobbyist, academic institutions and industry. Aleph Objects, Inc. has made both the LulzBot printers and corresponding software open source, allowing them to be modified for new applications. The LulzBot's combination of cost, being open source and availability made it a great candidate for this research.

A LulzBot TAZ 5, pictured below in figure 47, was used as the foundation for the UHTR 3D printing prototype. The original extruder was removed, and a screw extruder was retrofitted onto the printer so it could print the UHTR composite developed in previous work.

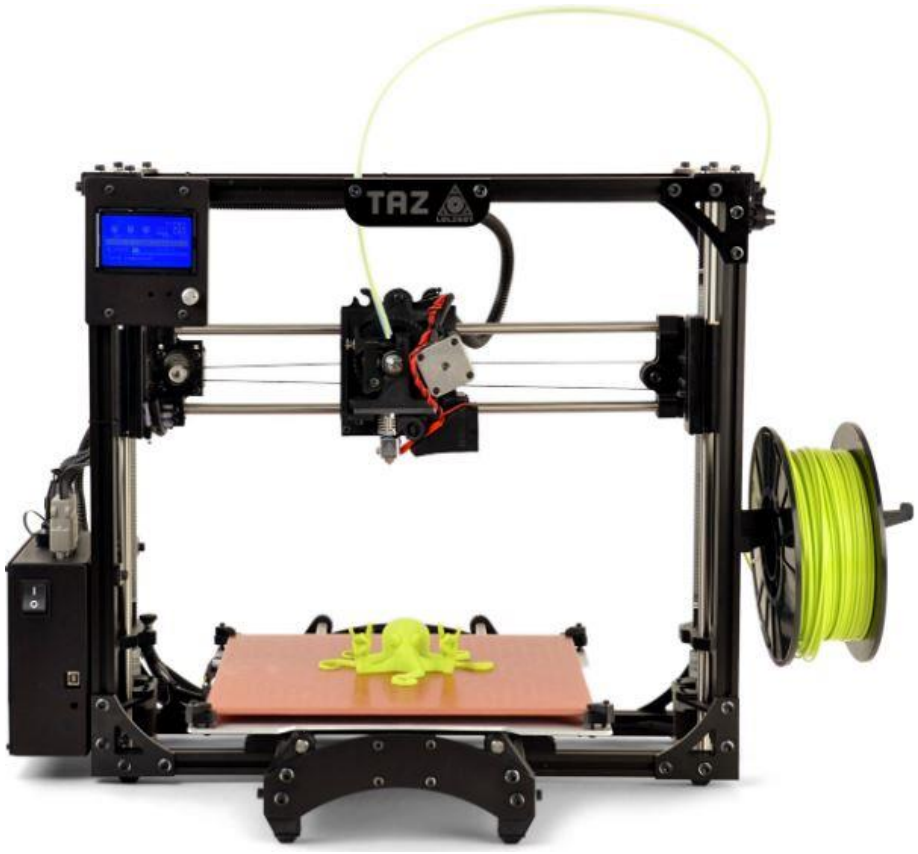

Figure 47 - LulzBot TAZ 5 3D Printer

Extrusion Mechanism

The extrusion mechanism is the most important aspect to the development of a UHTR composite 3D printing process. In initial research, the material system was tested for extrusion using syringes and they were the bases for the first extruder concept developed. Open source files were downloaded and used to print a syringe extruder similar to figure 46 above. The system was briefly tested but was quickly abandoned for a more scalable idea, an auger system. The initial auger prototypes were printed in the Ingram Hall Makerspace and used an Arduino to power the stepper motor that spins the auger. Due to printer limitations, these prototypes were not very accurate and had weak

tolerances. At this point the auger design was revaluated and a new more refined concept was developed.

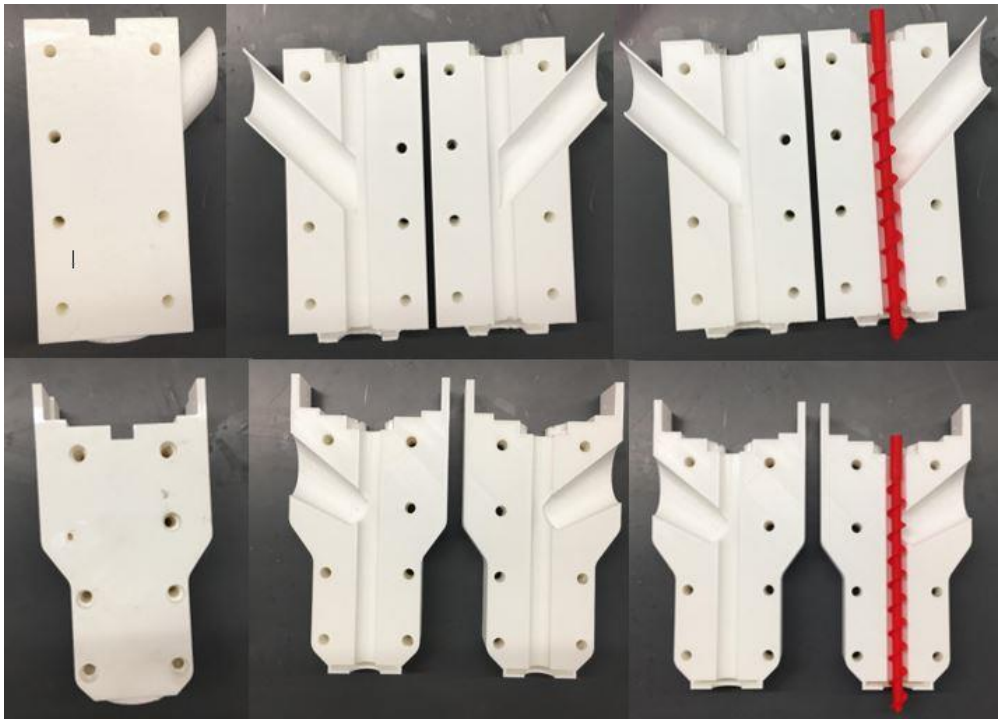

Figure 48 - Initial Auger Extruder Prototypes

Figure 48 above shows initial auger prototypes that were developed to connect to a stepper motor and Arduino board for a proof of concept. These were manufactured using the Craftbot FDM printers in the makerspace and printed out of PLA. They were low quality but gave a good foundation to build on.

Figure 49 - SolidWorks Model of the Auger Extruder

Using SolidWorks, a new design was developed for an auger extruder. The design incorporates intricate features like O-rings and tolerances must be tight to ensure no leakage of material and proper mating of components. The PLA printers in the makerspace were not ideal for this due to their limited accuracy so Dr. Asiabanpour, who runs the Rapid Product and Process Development (RPD) Center at Texas State was kind enough to make his Stratasys Objet260 Connex3 3D printer available for this research. The Objet uses the PolyJet printing process uses photopolymers that are jetted onto a build plate in thin layers and UV cured; this process is repeated until the final product is completed. The Objet260 is extremely accurate multi-material system that uses a wax support material to maintain the dimensional stability of the printed parts. The Objet260 in the RPD Center at Texas State is shown in figure 50.

Figure 50 - Stratasys Objet260 Connex3 3D Printer

Figure 51 below shows the final auger extruder design concept that was developed in SolidWorks. These models were later converted to STL files and printed with the Craftbot and Objet260 3D printers. Figure 52 shows the final printed assembly with the addition of the bearing, push-to-connect fitting and shaft coupling. The black "Bearing Retainer" was printed in PLA while the rest of the parts shown were printed in ABS on the Objet260.

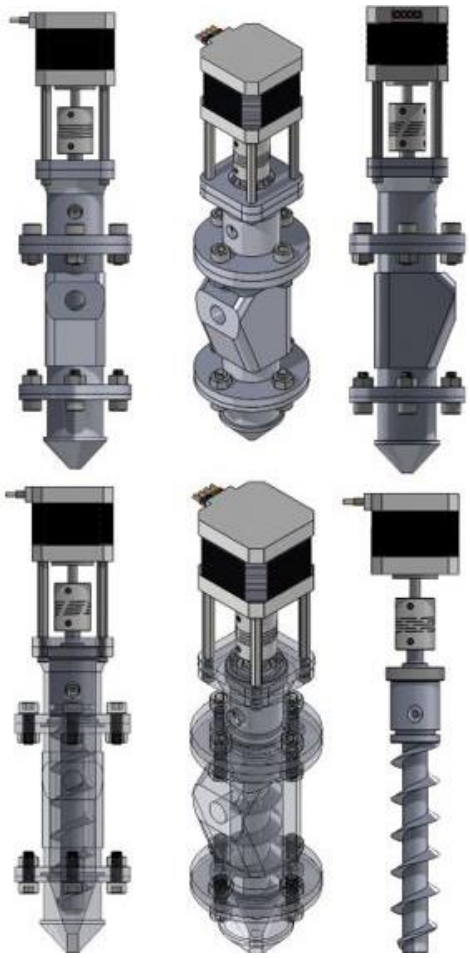

Figure 51 - SolidWorks Models of the Auger Extruder

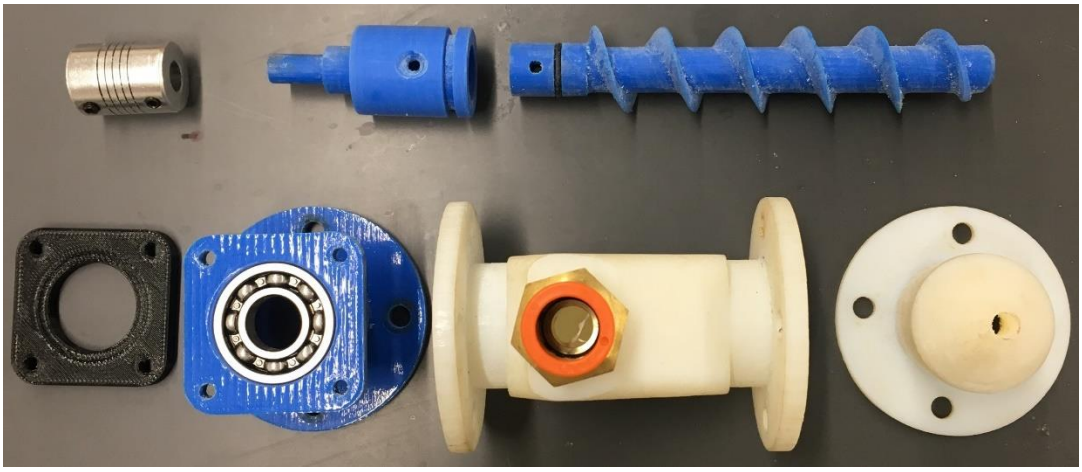

Figure 52 - 3D Printed Auger Extruder Components

Retrofitting the Auger Extruder

To mount the extrusion mechanism, some modifications were made to the LulzBot 3D printer. Since the new extruder was longer in the z-axis it would not home in that direction without running the nozzle into the print bed. The LulzBot uses bump stops for homing and an adjustable screw is used to hit the bump stop before the nozzle hits the bed. To compensate for the longer extruder, a piece was designed and 3D printed in the Texas State makerspace to extend the adjustable screw mount, it is shown in figure 53. The new piece fit seemlesly on the printer and was attached using existing mounting locations.

Figure 53 - Z-Axis Bump Stop Screw Extension

The new extruder was mounted to the printer using the legacy extruder's mounting location. A new mount was designed, and 3D printed in the Texas State makerspace. It took multiple iterations to get the design right, adjustments were made to the print infill and geometry to make sure the mount was strong enough to hold the

extruder and keep it stable. Iterations of the extruder mount are shown in figure 54 and the final mounting system is shown in figure 55.

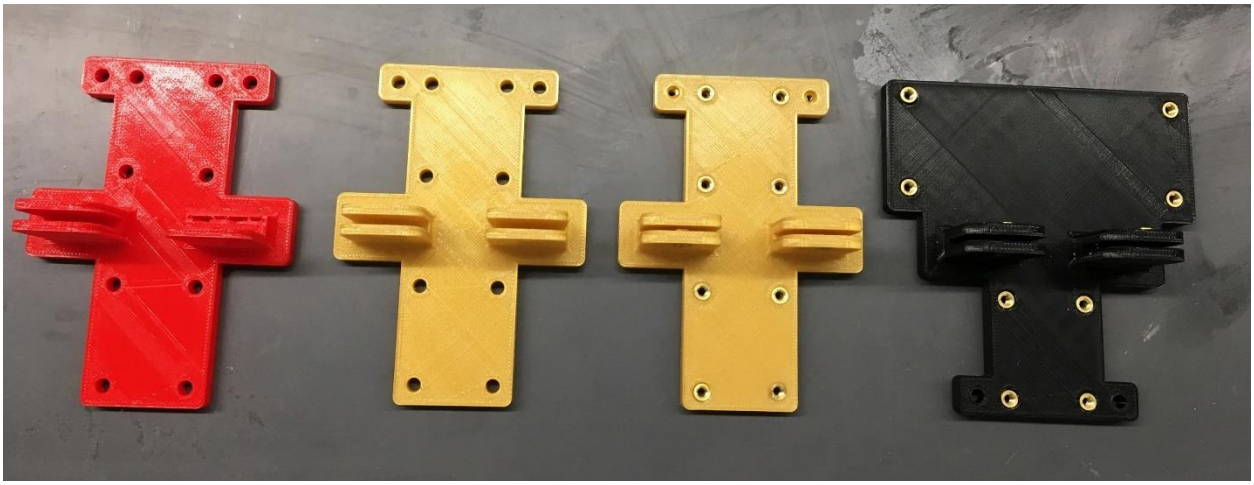

Figure 54 - Auger Extruder Mount Iterations

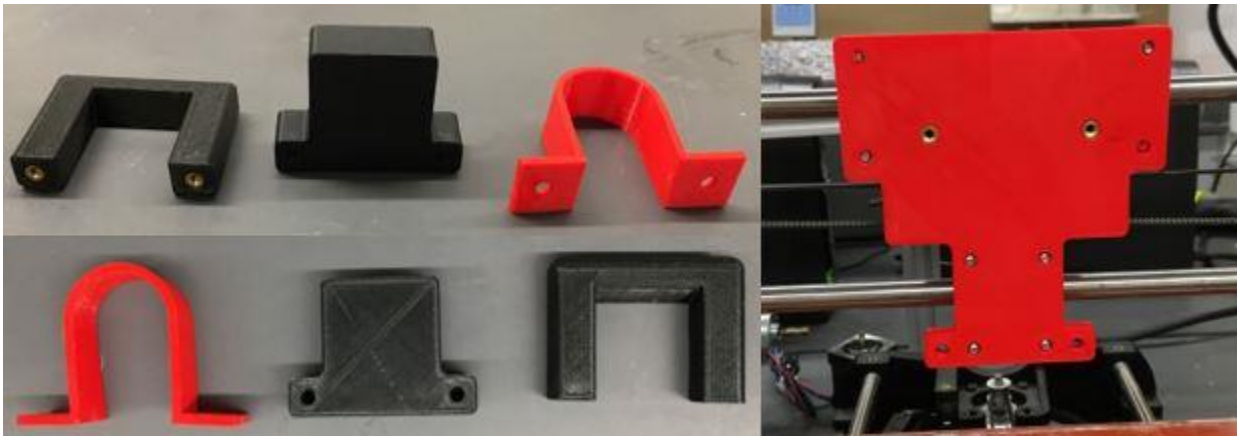

Figure 55 - Final Mounting Assembly for the Auger Extruder

Figure 56 shows the extruder mounted onto the LulzBot and figure 57 shows the final assembly of the retrofitted auger extruder.

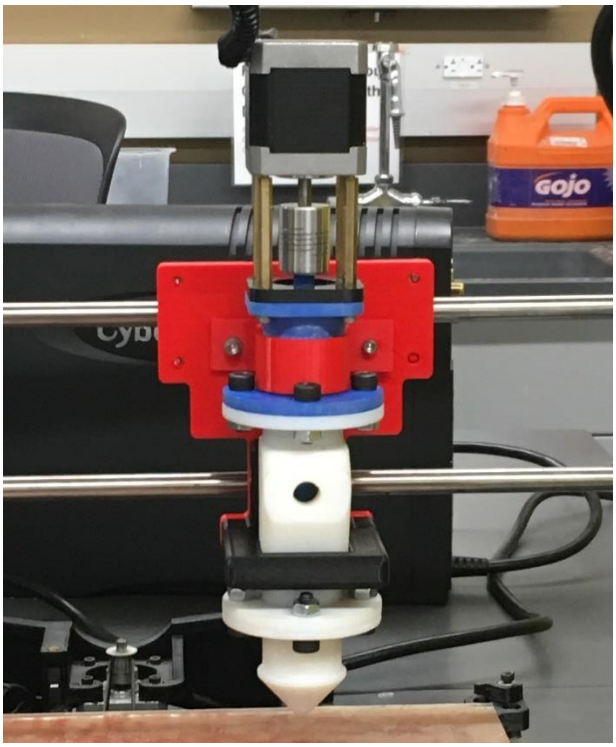

Figure 56 - Auger Extruder Assembly Attached to the LulzBot

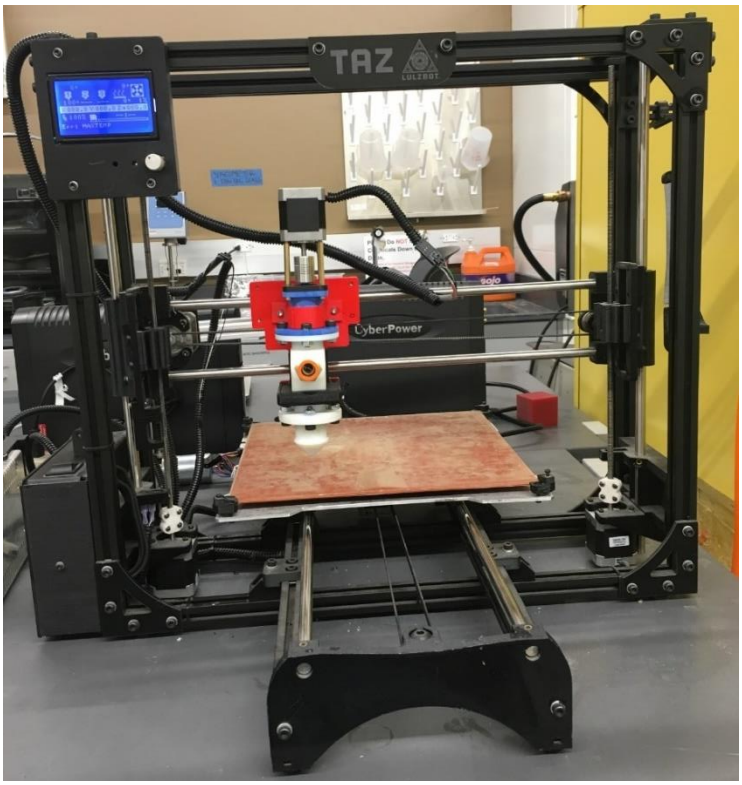

Figure 57 - Final Assembly of UHTR Printing 3D Printer

Material Delivery System

An important aspect of the 3D printing process is delivering the material to the extrusion mechanism. Due to its high viscosity, the UHTR composite needed some force behind it to move it along the desired path. To accomplish this, a Semco Model 250-A Gun with a 6oz capacity manufactured by PPG Industries was purchased. Semco guns are used for dispensing sealants, adhesives and other viscous materials in the aerospace industry. The Model 250-A is a pneumatic gun, powerful enough to move viscous fluids like UHTR with precision.

Figure 58 - Semco Model 250-A Gun

The extrusion mechanism was designed with a push-to-connect tube fitting so that it could be easily connected to the Semco gun. The Semco gun cartridges are threaded at the outlet so barbed fittings were simply threaded into them, making it easy to connect a hose from the Semco gun to the push-to-connect fitting on the auger extruder as shown in figure 59.

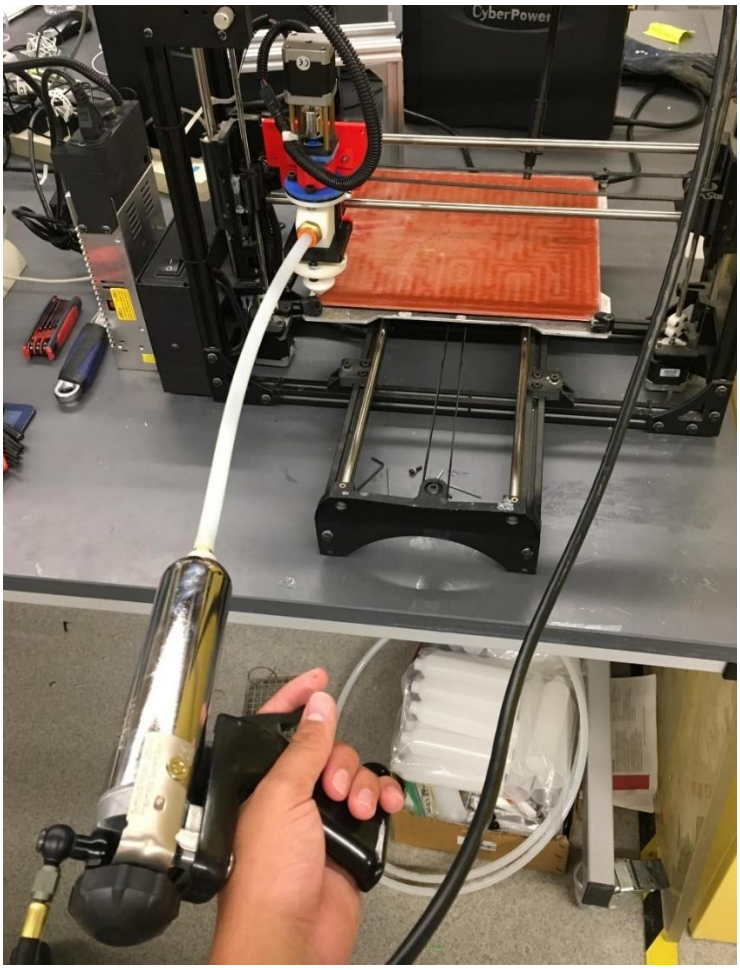

Figure 59 - Semco Gun Connected to the UHTR Extruder

Observations

After attaching the auger extruder to the LulzBot, it took some minor modifications to get it running effectively. The heating elements from the original extruder were disconnected from the motherboard along with the cooling fans. The thermistor was left connected to avoid a temperature error which would prevent prints from running. During testing, the printer would run the g-code and move in appropriate manner but the stepper controlling the auger screw would not spin. This was due to a

"cold extrusion" error caused by the thermistor only reading ambient temperatures. Most printers must reach the melting temperature of a material before the stepper controlling extrusion will run. This issue was solved by the addition of M302 into the g-code of the program that was being run. The M302 g-code allows for cold extrusion. The material delivery system needs to be fine tuned for this application. The air supplied to the lab is at 100 psi and seemed to overpower the auger in regards to pushing the material out. The air pressure and the stepper motor parameters need to be optimized for extruding the material system.

Future Work

The current UHTR printer will be used in future work to print specimens for mechanical and thermal evaluation. Ideally, the final printing concept will incorporate the catalyst at the optimal time before extrusion to create dimensional stability in printed parts as they are thermally cured. The entire system should be heated to reduce the viscosity of the UHTR material system to a manageable level for extrusion. A system that incorporates a continuous fiber into UHTR could present a solution to weak and brittle parts using short fibers and should be considered in future work. Future work should also focus on the material delivery system and what pressure to feed the material at. A regulator can be easily added to the system to control the air pressure. The effect of the printing parameters on the prints should be explored in depth so the optimum parameters can be determined for this material system. The addition of a geared stepper motor will likely be required to push the viscous slurry out without binding issues.

New formulations of UHTR using xylene have recently come out and they should be explored, as they may be more ideal for this application. Although it is not UV curable in its current form, UHTR may be able to be UV cured with the addition of photoinitiators and should be studied in future work.

VI. CONCLUSION

The goal of this research was to develop and characterize a material system consisting of Techneglas UHTR resin, milled carbon fiber and phenolic microballoons for 3D printing. This research is piece of a much larger project. UHTR resin has proven thermal properties when incorporated into fiber reinforcements, making it a promising ablative polymer matrix. To enhance the mechanical properties of the neat resin, milled carbon fibers were added, and the flexure strength was evaluated. The specimens are visibly weak, even with reinforcement and future work should focus on incorporating a continuous or significantly longer fiber into the resin system as opposed to dispersed fibers. The addition of phenolic microballoons allowed the material system to remain low density without compromising thermal properties, as supported in the TGA results. The microballoons do play a large role in the viscosity of the resin and should be thoughtfully incorporated.

Three different catalysts were evaluated in this research to determine if anyone stands out as the best option for 3D printing. Through a number of fundamental experiments, mechanical and thermal characterization, it was concluded that Geniosil GF 91 is the best overall choice at this time.

Throughout the trials of this research, lessons have been learned and many observations have been made regarding UHTR and its compatibility with additive manufacturing. UHTR is a very promising polymer, having great thermal properties specifically. It can be concluded from this research that UHTR is a viable option for 3D printing but its viscosity, inherent brittleness and poor mechanical performance with dispersed fillers are prominent issues. Inconsistencies with the resin, on the

manufacturing side, created issues with characterization and they must be solved to create a repeatable material system. The use of UHTR-F helped mitigate the quality issues seen in the IPA formulations and allowed more control over the resin's properties.

The culmination of this research has resulted in a foundation for future researchers to progress the characterization of the UHTR resin as well as 3D printing of thermoset resins for high-temperature applications.

REFERENCES

Bartlett E.P., Andrew L.W., Curry D.M. An evaluation of ablation mechanisms for the Apollo heat shield material. J Spacecraft Rock 1971;8:463-9

Bennett, J. (2017). Measuring UV curing parameters of commercial photopolymers used in additive manufacturing. Additive Manufacturing, 18, 203-212. doi:10.1016/j.addma.2017.10.009

Boghozian, T., M. Stackpoole, and G. Gonzales, Alternative High Performance Polymers for Ablative Thermal Protection Systems. 2015

Clark, S. (2014, November 05). Engineers recommend changes to Orion heat shield. Retrieved from https://spaceflightnow.com/2014/11/05/engineers-recommend-changes-to-orion-heat-shield/

Colombo, P., Schmidt, J., Franchin, G., Zocca, A., & Gunster, J. (n.d.). Additive manufacturing techniques for fabricating complex ... Retrieved from http://ceramics.org/wp-content/uploads/2017/03/April2017_feature.pdf

DIMITRIENKO, Y. I. (2018). *THERMOMECHANICS OF COMPOSITE STRUCTURES UNDER HIGH TEMPERATURES*. S.l.: SPRINGER.

Formalev, V. F., Kolesnik, S. A., Kuznetsova, E. L., & Rabinskii, L. N. (2016). Heat and mass transfer in thermal protection composite materials upon high temperature loading. *High Temperature*,*54*(3), 390-396. doi:10.1134/s0018151x16020036

Franchin, G., Maden, H., Wahl, L., Baliello, A., Pasetto, M., & Colombo, P. (2018). Optimization and Characterization of Preceramic Inks for Direct Ink Writing of Ceramic Matrix Composite Structures. *Materials*,*11*(4), 515. doi:10.3390/ma11040515

Gotro, J. (2016, February 29). UV Curing Part Eight: With Great Power Comes Great Responsibility [Web log post]. Retrieved from https://polymerinnovationblog.com/uv-curing-part-eight-great-power-comes-great-responsibility/

Herridge, L. (2018, August 16). Heat Shield Install Brings Orion Spacecraft Closer to Space. Retrieved from https://www.nasa.gov/feature/heat-shield-install-brings-orion-spacecraft-closer-to-space

Jia, X., Li, P., Yu, Y., Sui, G., Huang, Z., Li, G., et al. (2010). Effects of pre-dispersed hollow phenolic micro-spheres on properties of EPDM thermal insulator and study on functionally graded thermal insulator. *Journal of Solid Rocket Technology*,*33,* 99-103.

Khoshnevis, B. (2004). Automated construction by contour crafting—related robotics and information technologies. Automation in Construction, 13(1), 5-19. doi:10.1016/j.autcon.2003.08.012

McDermott, R. (2018). *Exploration of a New Affordable Thermal Protection System Utilizing Needle-Punched (2.5D) Fabric Composites*. Texas State University, San Marcos, Texas

Natali, M., Puri, I., Kenny, J. M., Torre, L., & Rallini, M. (2017). Microstructure and ablation behavior of an affordable and reliable nanostructured Phenolic Impregnated Carbon Ablator (PICA). Polymer Degradation and Stability, 141, 84-96. doi:10.1016/j.polymdegradstab.2017.05.017

Natali, M., Kenny, J. M., & Torre, L. (2016). Science and technology of polymeric ablative materials for thermal protection systems and propulsion devices: A review. *Progress in Materials Science,84*, 192-275. doi:10.1016/j.pmatsci.2016.08.003

Permal, A., Devarajan, M., Hung, H. L., Zahner, T., Lacey, D., & Ibrahim, K. (2017). Improved thermal and mechanical properties of aluminium oxide filled epoxy composites by reinforcing milled carbon fiber by partial replacement method. Journal of Materials Science: Materials in Electronics, 28(18), 13487-13495. doi:10.1007/s10854-017-7188-8

PICA Material Property Report for Crew Exploration Vehicle Block II Heatshield Advanced Development Project (2009), in *NASA Report CEV TPS ADP, C-TPSA-A-DOC-158*, Rev. 1.

Schellhase, K. J., Koo, J. H., Wu, H., & Buffy, J. J. (2018). Experimental Characterization of Material Properties of Novel Silica/Polysiloxane Ablative. *Journal of Spacecraft and Rockets,*1-13. doi:10.2514/1.a34044

Schellhase, K. J., Koo, J. H., Buffy, J. J., Wu, H., & Lui, E. (2017). Development of New Thermal Protection Systems Based on Silica/Polysiloxane Composites: Properties Characterization II. *SAMPE Conference Proceedings*

Silva, H. P., Pardini, L. C., & Bittencourt, E. (2016). Shear Properties of Carbon Fiber/Phenolic Resin Composites Heat Treated at High Temperatures. *Journal of Aerospace Technology and Management,8*(3), 363-372. doi:10.5028/jatm.v8i3.643

Strong, A. B. (2008). *Fundamentals of composites manufacturing: Materials, methods and applications*. Place of publication not identified: Society of Manufacturing Engineers.

Torre, L., Kenny, J. M., Boghetich, G., & Maffezzoli, A. M. (2000). Degradation behaviour of a composite material for thermal protection systems Part III–Char characterization. *Journal of Materials Science,33*(12), 3137-3143. doi:10.1023/a:1004399923891

Torre, L., Kenny, J. M., & Maffezzoli, A. M. (1998). Degradation behaviour of a composite material for thermal protection systems Part I–Experimental characterization. *Journal of Materials Science,35*, 4563-4566.

T. (n.d.). 60ml Syringe Extruder for Liquid Deposition Modeling - LDM by piuLAB. Retrieved from https://www.thingiverse.com/thing:482873

Vitug, E. (2016, March 29). First 3D woven composite for NASA thermal protection systems. Retrieved from https://www.nasa.gov/feature/first-3d-woven-composite-for-nasa-thermal-protection-systems

Warga, J. J. (1970). Low-Cost Fabrication Techniques For Solid Rocket Nozzles. *SAE Technical Paper Series*. doi:10.4271/700796

Zhang, J., & Jung, Y. (2018). *Additive manufacturing: Materials, processes, quantifications and applications*. Cambridge, MA: Butterworth-Heinemann.

Zhao, X., Song, L., Zhu, X., Liu, K., Zang, C., Wen, Y., & Jiao, Q. (2018). One-step enrichment of silica nanoparticles on milled carbon fibers and their effects on thermal, electrical, and mechanical properties of polymethyl-vinyl siloxane rubber composites. Composites Part A: Applied Science and Manufacturing, 113, 287-297. doi:10.1016/j.compositesa.2018.08.001

ZOLTEK Products. (n.d.). Retrieved from http://zoltek.com/products/px35/